

Simulating the evolution of disc galaxies in a group environment. I. The influence of the global tidal field

Á. Villalobos^{1*}, G. De Lucia¹, S. Borgani^{1,2,3}, and G. Murante⁴

¹*INAF - Astronomical Observatory of Trieste, via G.B. Tiepolo 11, I-34143 Trieste, Italy*

²*Astronomy Unit, Department of Physics, University of Trieste, via G.B. Tiepolo 11, I-34131 Trieste, Italy*

³*INFN - Istituto Nazionale di Fisica Nucleare, Trieste, Italy*

⁴*INAF - Istituto Nazionale di Astrofisica - Osservatorio Astronomico di Torino, Str. Osservatorio 25, I-10025, Pino Torinese, Torino, Italy*

2 September 2018

ABSTRACT

We present the results of a series of numerical simulations aimed to study the evolution of a disc galaxy within the global tidal field of a group environment. Both the disc galaxy and the group are modelled as multi-component, collision-less, N -body systems, composed by both dark matter and stars. In our simulations, the evolution of disc galaxies is followed after they are released from the group virial radius, and as their orbits sink towards the group centre, under the effect of dynamical friction. We explore a broad parameter space, covering several aspects of the galaxy-group interaction that are potentially relevant to galaxy evolution. Namely, prograde and retrograde orbits, orbital eccentricities, disc inclination, role of a central bulge in discs, internal disc kinematics, and galaxy-to-group mass ratios. We find that significant disc transformations occur only after the mean density of the group, measured within the orbit of the galaxy, exceeds ~ 0.3 –1 times the central mean density of the galaxy. The morphological evolution of discs is found to be strongly dependent on the initial inclination of the disc with respect to its orbital plane. That is, discs on face-on and retrograde orbits are shown to retain longer their disc structures and kinematics, in comparison to prograde discs. This suggests that after interacting with the global tidal field alone, a significant fraction of disc galaxies should be found in the central regions of groups. Prominent central bulges are not produced, and pre-existing bulges are not enhanced in discs after the interaction with the group. Assuming that most S0 are formed in group environments, this implies that prominent bulges should be formed mostly by young stars, created only after a galaxy has been accreted by a group. Finally, contrary to some current implementations of tidal stripping in semi-analytical models of galaxy evolution, we find that more massive galaxies suffer more tidal stripping. This is because dynamical friction brings them faster to the group centre, in comparison to their lower mass counterparts.

Key words: galaxies: evolution – galaxies: structure – galaxies: kinematics and dynamics – galaxies: interactions – methods: N-body simulations

1 INTRODUCTION

Galaxies in high density environments, such as clusters or groups, have properties that are consistently different from those of galaxies in regions of the Universe with “average” density. For instance, in comparison to field galaxies, the population of galaxies within groups and clusters is characterised by a higher fraction of red galaxies with lower average star formation rate, as well as by a lower fraction of disc galaxies (e.g., Dressler et al. 1997;

Lewis et al. 2002; Gómez et al. 2003; Balogh et al. 2004; Weinmann et al. 2006; McGee et al. 2008). Although the precise mechanisms responsible for such differences remain unknown, these observational findings do highlight the key role played by environment in the evolution of galaxies.

In the framework of the currently favoured cosmological model (the Λ CDM model), galaxy clusters are formed at relatively late times, through a series of mergers and accretion events of both dark matter and baryonic material, ranging from small halos, isolated galaxies to large galaxy groups. In such a context, a galaxy that resides in a cluster at present-time has experienced several different environments dur-

* villalobos@oats.inaf.it

ing its lifetime (e.g., Lacey & Cole 1994; Zhao et al. 2003; Berrier et al. 2009; McGee et al. 2009). In each of these environments, a galaxy might have been affected by different physical processes, such as, strangulation, ram-pressure stripping, as well as tidal forces against the background potential, and close encounters with other galaxies and substructures orbiting within the same dark matter halo. The combined effect of these processes likely played a significant role in shaping the observed physical properties of galaxies residing in groups and clusters at present time (see the review by Weinmann et al. 2011b). Thus, in order to better understand the origin of these properties, it is crucial to characterise and quantify the relative effect that those physical processes have on galaxies, in different environments.

From a theoretical point of view, a number of studies have used numerical N -body simulations to investigate the influence of environments on galaxy evolution. Most of them, however, have been focused either on cluster mass scales (e.g., Moore et al. 1999; Gnedin 2003; Mastropietro et al. 2005), or on Milky Way-like mass scales (e.g., Mayer et al. 2001a,b; Klimontowski et al. 2009; Kazantzidis et al. 2011). For example, Mastropietro et al. studied the influence of tidal stripping and galaxy harassment on the evolution of disc galaxies within a cluster environment. In their study, the authors extracted a cluster environment from a cosmological simulation, and replaced 20 of its particles (randomly chosen at redshift $z=0.5$) with high-resolution multi-component galaxy models. The authors found that the cluster environment induces a series of strong bar formation episodes that transform the galaxy morphologies from late-type discs to dwarf spheroidals. The galaxies retain, however, a significant fraction of their rotational motion. Other authors have taken advantage of hydrodynamic simulations, using either smoothed-particle hydrodynamics (SPH) or grid codes, to study the removal of a galaxy’s gas disc during its motion through the intracluster medium (Quilis et al. 2000; Roediger & Brüggen 2006). At the lower end of the mass spectrum, in a recent study, Kazantzidis et al. (2011) examined the transformation of dwarf disc galaxies into dwarf spheroidals, driven by tidal interactions with a Milky Way-size host galaxy, using N -body simulations of self-consistent stellar discs placed within cosmologically motivated dark matter (DM) halos.

On the group mass scale, some studies have explored the role played by ram pressure stripping in the evolution of galaxies that move through an intragroup medium (e.g., Marcolini et al. 2003; Roediger & Hensler 2005; Tecce et al. 2011), while recent work has focused on the evolution of dwarf galaxies in the Local Group (Sawala et al. 2011), and on the transformation of spiral galaxies into S0 galaxies via repeated close encounters with other group galaxies (Bekki & Couch 2011). Overall, surprisingly little work has been dedicated so far to systems with velocity dispersions typical of galaxy groups, even though they arguably represent the most common environment that galaxies experience. Indeed, it has long been claimed that a significant fraction of the cluster galaxy population might have been “pre-processed” in groups, that later merged onto clusters (Zabludoff & Mulchaey 1998). This appears to be confirmed by McGee et al. (2009, but see also Berrier et al. 2009), who used merger tree information from semi-analytic catalogues to explore the accretion of galaxies onto clusters and groups.

The authors found that clusters at redshift epochs ranging from $z=0$ to $z=1.5$ have accreted a significant fraction of galaxies through groups. Specifically, they estimated that ~ 40 per cent of galaxies with $M_{\text{stellar}} > 10^9 M_{\odot}$ were accreted onto clusters with $M_{\text{cluster}} = 10^{14.5} M_{\odot}$ through groups with $M_{\text{group}} > 10^{13} M_{\odot}$. In a recent paper, De Lucia et al. (2011) confirm that a significant fraction of the galaxies that currently reside in a cluster have spent time as satellites of a lower mass system before being accreted onto the final parent halo. This fraction is largest for lowest mass galaxies. In addition, by comparing their theoretical predictions with observational estimates of the passive fraction as a function of the parent halo mass and cluster-centric radius, they argue that satellite galaxies become passive after they have spent a relatively long time ($\sim 5 - 7$ Gyr) in halos more massive than $\sim 10^{13} M_{\odot}$. It is therefore crucial to understand the influence of different physical processes on galaxy evolution for scales typical of galaxy groups.

The aim of this paper is to help alleviate the aforementioned lack of numerical studies by exploring the evolution of disc galaxies within a group environment, covering a broad parameter space. We use high-resolution N -body simulations and focus specifically on the effect of the global tidal forces on galaxy evolution. This approach allows us to isolate this effect, distinguishing it from those of other relevant processes, such as, low-velocity close encounters with other group members. Ultimately, we plan a better quantification of the relative importance that different physical process have on galaxy evolution, as they are gradually introduced in the next papers of this series. Because of this approach, our group environments are built from idealised initial conditions, do not account for hierarchical growth, and do not contain substructures. Thus, by design, the simulations presented in this study do not include the effect of close encounters on galaxy evolution.

The layout of this paper is as follows: §2 describes the set-up of our experiments; §3 describes the results of our simulations; in §4 we discuss our results and in §5 we summarise our conclusions. At the end of each subsection in §3 we include short summaries for readers who prefer to skip the detailed description of the simulations.

2 SET-UP OF NUMERICAL EXPERIMENTS

We have carried out a total of 17 experiments in order to study the general evolution of disc galaxies within a group environment. Our basic strategy is to release a single disc galaxy at a time, from the virial radius of the group, studying the evolution of its morphology and kinematics as it orbits within the group. Each experiment explores a single aspect of the galaxy-group interaction (see below), in order to estimate its role in the general evolution of galaxies. We run our simulations for 12 Gyr, independently of whether the galaxy reaches the centre of the group, it is destroyed or it survives.

The group environment is modelled as a N -body (i.e. “live”) DM halo, following a NFW density profile (Navarro et al. 1997):

$$\rho_{\text{halo}}(r) = \frac{\rho_s}{(r/r_s)(1+r/r_s)^2}, \quad (1)$$

Table 1. Properties of group environments.

	“z=0”	“z=1”	
DM Halo			
Virial mass	9.9×10^{12}	9.9×10^{12}	(M_{\odot})
Virial radius	555.94	329.19	(kpc)
Concentration	9.74	4.87	
Circular velocity	276.97	360.07	(km s^{-1})
Number particles	1.1×10^6	1.1×10^6	
Softening	0.55	0.32	(kpc)
Stellar spheroid			
Mass	10^{11}	10^{11}	(M_{\odot})
Scale radius	3.24	1.91	(kpc)
Number particles	5×10^5	5×10^5	
Softening	0.1	0.06	(kpc)

Table 2. Properties of disc galaxies.

Label experiment	“z=0”			“z=1”			
	REF,BUL ⁽¹⁾ ,CIR, RAD,RET,COL ⁽²⁾ ,FON	MR1:5	MR1:20	REF,BUL ⁽¹⁾ ,CIR, RAD,RET,COL ⁽²⁾ ,FON	MR1:10	MR1:40	
DM Halo							
Virial mass	10^{12}	2×10^{12}	5×10^{11}	5.07×10^{11}	10^{12}	2.53×10^{11}	(M_{\odot})
Virial radius	258.91	326.2	205.5	122.22	153.98	97	(kpc)
Concentration	13.12	11.99	14.36	6.56	6	7.18	
Circular velocity	129.17	162.76	102.51	133.93	168.77	106.29	(km s^{-1})
Number particles	5×10^5	5×10^5	5×10^5	10^6 ⁽³⁾	10^6	10^6	
Softening	0.35	0.44	0.28	0.41	0.6	0.6	(kpc)
Stellar disc							
Disc mass	2.8×10^{10}	5.6×10^{10}	1.4×10^{10}	1.42×10^{10}	2.84×10^{10}	7.09×10^9	(M_{\odot})
Scale-length	3.5	4.4	2.7	1.6	1.6	1.6	(kpc)
Scale-height	0.35	0.44	0.27	0.16	0.16	0.16	(kpc)
Q	2	2	2	2.5 ⁽³⁾	2	3	
Number particles	10^5	10^5	10^5	10^5	10^5	10^5	
Softening	0.05	0.06	0.04	0.012	0.012	0.012	(kpc)

(1): A stellar bulge is added at the centre of the disc, with $M_{\text{bulge}}=0.3M_{\text{disc}}$ and $a_{\text{bulge}}=0.2R_{\text{D}}$. (2): Disc kinematically cold, with $Q=1.25$. (3): Values are larger, with respect to “z=0”, to enhance the stability of the disc against the formation of a bar.

where ρ_s is a characteristic scale density and r_s a scale radius. The simulated group also includes a spherically symmetric stellar component at its centre to account for a central galaxy, that is assumed to follow a Hernquist density profile (Hernquist 1990):

$$\rho_*(r) = \frac{M_*}{2\pi} \frac{a_*}{r(r+a_*)^3}, \quad (2)$$

where M_* is the stellar mass and a_* is the scale radius. Galaxies are modelled as multi-component systems composed by a stellar disc embedded in a DM halo. Stellar discs are built according to the following density profile:

$$\rho_{\text{disc}}(R, z) = \frac{M_{\text{disc}}}{8\pi R_{\text{D}}^2 z_{\text{D}}} \exp\left(-\frac{R}{R_{\text{D}}}\right) \text{sech}^2\left(\frac{z}{2z_{\text{D}}}\right), \quad (3)$$

where M_{disc} is the disc mass, R_{D} is the exponential scale-length, and z_{D} is the exponential scale-height. Depending on the experiment, the stellar discs can also contain a central stellar bulge, following a Hernquist profile. Galaxy DM ha-

los follow a NFW density profile and are initially spherical, do not rotate, and the structure of their inner region has been adiabatically contracted to account for the growth of the baryonic component(s). We refer the interested reader to Villalobos & Helmi (2008) for a complete description of the procedure followed to generate the self-consistent initial conditions used for this study.

Our experiments probe an ample range of the parameter space, exploring different aspects of the galaxy-group interaction that are potentially relevant to the evolution of galaxies. In particular, we study the effect of: prograde and retrograde infalls (with respect to the sense of rotation of the disc), different orbital eccentricities, the presence of a central stellar bulge in the disc, different internal kinematics of the disc, and different galaxy-to-group mass ratios. The initial orbital parameters of discs are chosen to be consistent with distributions of orbital parameters of infalling substructures, obtained from cosmological simulations (Benson 2005). In

Table 3. List of experiments at redshift “ $z=0$ ” [and “ $z=1$ ”].

Label	Orbit (1)	θ^a (2)	$(V_r, V_\phi)^a$ (3)	e^a (4)	$M_{\text{galaxy}}:M_{\text{group}}$ (5)	Notes (6)
REF	Prograde	0°	(0.9,0.6)	0.86	1:10 [1:20]	Reference experiment
BUL	Prograde	0°	(0.9,0.6)	0.86	1:10 [1:20]	Bulge added to disc
CIR	Prograde	0°	(0.6,1.1)	0.6	1:10 [1:20]	More “circular” infall
RAD	Prograde	0°	(1.2,0.3)	0.97	1:10 [1:20]	More “radial” infall
RET	Retrograde	180°	(0.9,0.6)	0.86	1:10 [1:20]	Retrograde orbital infall
FON	-	90°	(0.9,0.6)	0.86	1:10 [1:20]	“Face-on” infall
COL	Prograde	0°	(0.9,0.6)	0.86	1:10	“Colder” disc kinematics
MR1:5 [MR1:10]	Prograde	0°	(0.9,0.6)	0.86	1:5 [1:10]	More massive galaxy
MR1:20 [MR1:40]	Prograde	0°	(0.9,0.6)	0.86	1:20 [1:40]	Less massive galaxy

(1) Sense of the orbital infall with respect to the disc rotation. (2) Initial angle between the orbital and intrinsic angular momentum of the disc. (3): Radial and tangential components of the initial velocity of the disc, in units of the virial circular velocity of the group. (4): Initial orbital eccentricity. (5): Initial galaxy-to-group mass ratio. (6): Differences with respect to the reference experiment. (a): Same values used at both redshift epochs.

order to cover those distributions, we choose for our experiments the most likely eccentricity of infall, and both the least and the most eccentric orbits.

We place our simulations at two different redshift epochs, “ $z=0$ ” and “ $z=1$ ”¹. Thus, we are able to also explore possible dependencies of disc evolution on the group structure. We choose to use a fixed value for the mass of groups at both “ $z=0$ ” and “ $z=1$ ” ($10^{13}M_\odot$, that is within the mass range reported by McGee et al. 2009 where significant environmental effects must take place), only evolving with redshift both the group concentration and virial radius.

At each redshift, we define our “reference” galaxy models as those with bulge-less discs, on prograde infalling orbits with the most likely orbital eccentricity. At “ $z=0$ ” the reference galaxy resembles a bulge-less, slightly less massive Milky Way (MW), while at “ $z=1$ ” it is a smaller version of the MW, obtained by scaling down its properties as in Mo, Mao, & White (1998). This scaling involves defining both the disc mass and the disc scale-length as constant fractions of the virial mass and virial radius of the galaxy halo, respectively, at each redshift. Therefore, our reference galaxy at “ $z=1$ ” is half as massive as that at “ $z=0$ ”. Tables 1 and 2 list the structural parameters of our groups and disc galaxies, respectively, and Table 3 provides the complete list of experiments and their characteristics. Throughout the paper we refer to each experiment by its label or its main characteristic interchangeably.

We have also performed simulations of all disc galaxies in isolation, evolving them as long as the full simulations, 12 Gyr. Our galaxies are found to be stable, in terms of their structure and kinematics, and show a negligible evolution in

the conservation of both their total energy and total angular momentum.

The typical computational cost required to complete a single simulation is between 432 and 768 core processor hours, using 32 tasks (i.e., 16 cores in simultaneous multi-threading mode) of the IBM P575 Power 6 (“SP6”) supercomputer hosted by CINECA². The simulations were run using GADGET-3, a non-public evolution of the GADGET-2 code. We refer the interested reader to Springel (2005), for a complete description of the latter. The main improvement of GADGET-3 over GADGET-2 resides in its multiple domain decomposition. Domain decomposition in the GADGET code is based on the computation of the Peano-Hilbert space-filling curve connecting all the particles. This curve is then split into M segments, to be assigned to different processors. These segments are then ranked according to their estimated computational cost. In the GADGET-3 code, each of the N ($<M$) tasks is allowed to receive more than one disjointed segment of the Peano-Hilbert curve, with the first task receiving the most and the least expensive, and so on, thus providing a more efficient work-load balance among the tasks. This kind of decomposition allows a substantial increase in speed, especially when a few massive objects dominate the processing cost, as in the simulations presented here.

3 RESULTS

3.1 Disc orbital evolution

In our simulations, the evolution of the disc galaxies takes place from the moment they are released on an infalling or-

¹ The quotation marks denote that our group environments are not evolved with cosmic time throughout the simulations.

² <http://hpc.cineca.it/>.

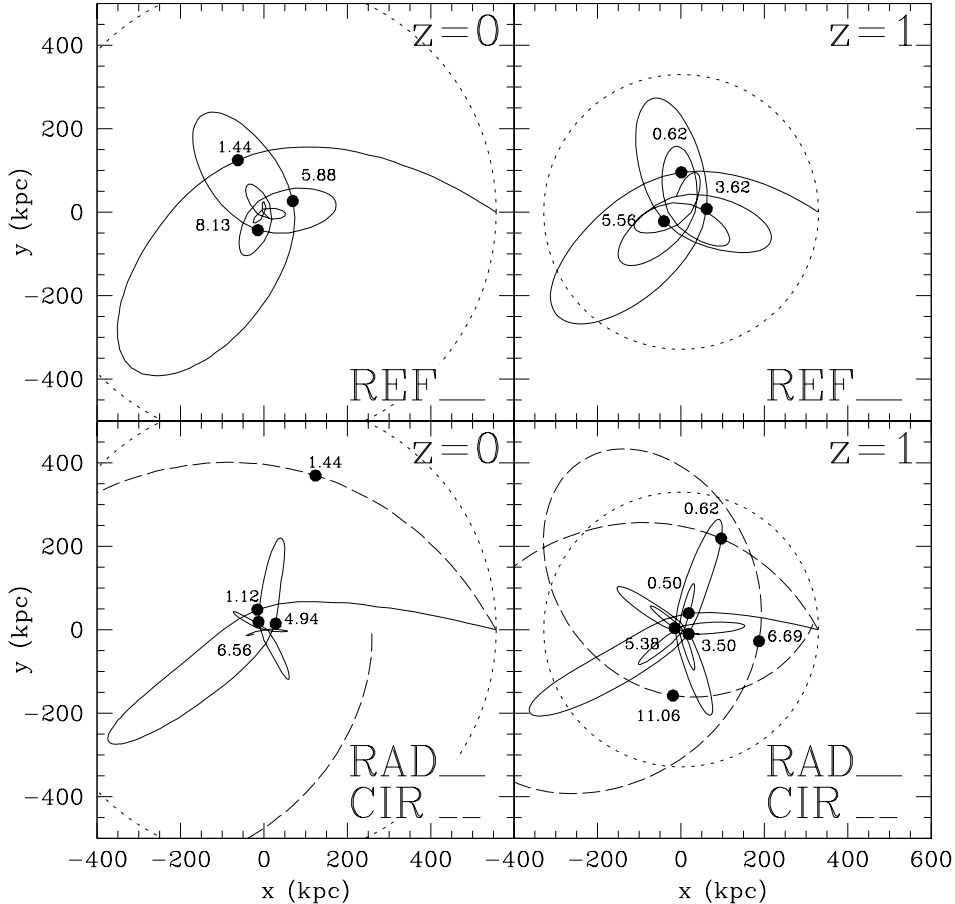


Figure 1. Trajectories of the centres of mass of disc galaxies with initial orbital eccentricities $e=0.86$, 0.6 and 0.97 (REF, CIR and RAD experiments, respectively), as they spiral in towards the centre of the group at redshift “ $z=0$ ” and “ $z=1$ ”. The coordinate system is centred on the centre of mass of the group and the XY projections are on the orbital plane of the disc. The first pericentric passages (solid dots), and their respective times (in units of Gyr), are included as reference, as well as the initial virial radius of the group (dotted lines).

bit at the virial radius of the group environment. Figure 1 shows the trajectories, over 12 Gyr of infall, of the centre of mass of the disc galaxy for our REF (reference), RAD (most radial infall) and CIR (most circular infall) experiments for the redshift epochs “ $z=0$ ” and “ $z=1$ ”. This figure offers a direct comparison between the most likely orbit of infall, according to velocity distributions from cosmological simulations, and the extremes of those distributions. At a given redshift epoch, the most likely orbit seems more similar to the most radial infall than to the most circular one. This can also be noted in terms of the initial eccentricities of the orbits (see Table 3). However, in the most radial orbit, the disc galaxy penetrates deeper in the central region of the group and on shorter timescales than in the case of the most likely orbit. Thus, the disc galaxy on a more radial orbit is affected faster by stronger tidal shocks against the central potential of the group. This leads to a more dramatic evolution in the disc, especially with respect to a more circular orbit in which the disc galaxy experiences fewer pericentric passages, generally closer to the virial radius of the group than to its centre.

The disc galaxy on the most likely infalling orbit at “ $z=1$ ” experiences more pericentric passages in comparison to the same case at “ $z=0$ ”. This is expected as a consequence of the smaller galaxy-to-group mass ratio at “ $z=1$ ” (1:20 vs. 1:10), which is inversely proportional to the merging timescale driven by dynamical friction. In general, in our experiments at “ $z=1$ ”, the disc galaxy spends more time away from the denser central region of the group, as opposed to “ $z=0$ ”, meaning that the disc is exposed to a broader range of mostly lower densities within the group. In fact, for the most circular orbit at “ $z=1$ ”, the galaxy spends a significant amount of time beyond the (initial) virial radius of the group.

The strong influence of dynamical friction on the infalling disc galaxy, that progressively shrinks its orbit over time, is evident in Figure 1. Dynamical friction is usually understood as the dragging force exerted on an object that moves through a homogeneous medium, which in N -body simulations is usually modelled by numerous less massive particles. Such dragging force comes from the gravitational pull produced by medium particles, that cluster behind the

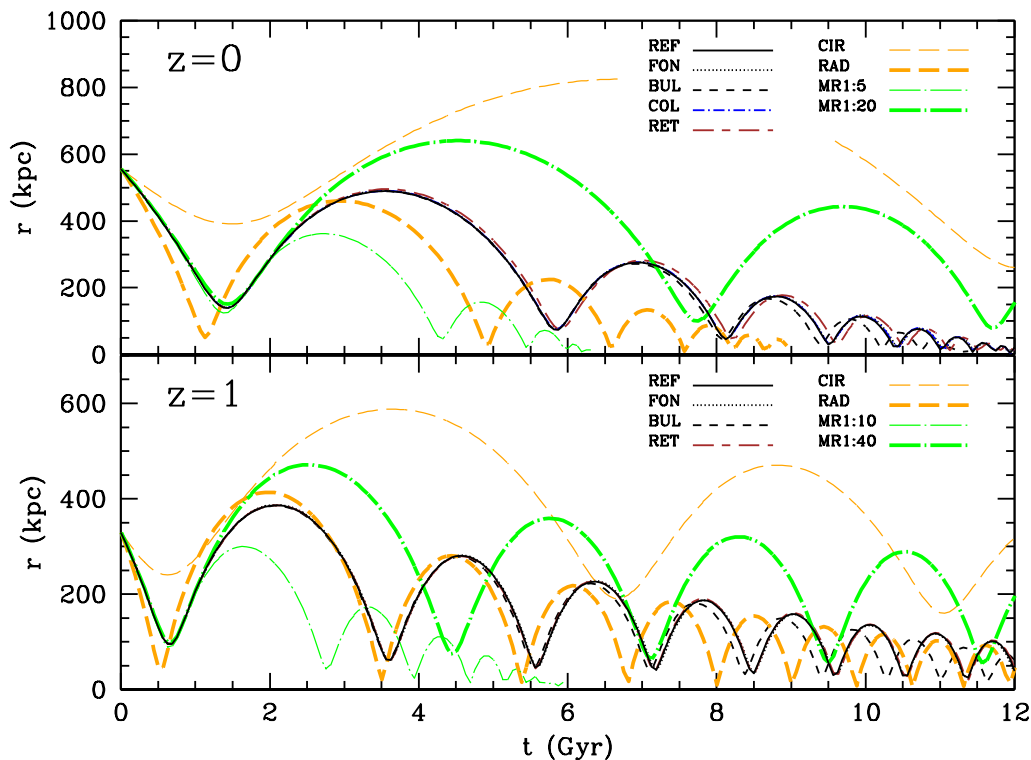


Figure 2. Evolution of the distance between the centres of mass of the disc and that of the group for all our experiments, at redshift epochs “ $z=0$ ” and “ $z=1$ ”.

moving object. As it can be seen in our experiments, such dragging force continuously reduces the galaxy tangential velocity (and angular momentum), causing it to spiral-in towards the centre of the group. This can also be seen in Figure 2 as a monotonic decrease of both the apocentric and pericentric distances, over subsequent passages of the disc galaxy around the centre of the group. Figure 2 also shows the dependence of dynamical friction on the initial orbital parameters of the disc galaxy and on the galaxy-to-group mass ratio. Dynamical friction is less efficient for orbits that are initially more circular (CIR vs. REF vs. RAD), and also for lower galaxy-to-group mass ratio (MR1:20 vs. REF vs. MR1:5, for “ $z=0$ ”; MR1:40 vs. REF vs. MR1:10, for “ $z=1$ ”). The first trend can be understood in terms of the radial mass distribution of the group. A disc galaxy initially on a more circular infalling orbit spends more time at larger distances from the centre of the group, where the medium surrounding the galaxy is less dense. Therefore, it is less efficient at dragging the disc galaxy and reducing its angular momentum. The second trend, as mentioned above, accounts for the inverse proportionality between the galaxy-to-group mass ratio and the timescale of dynamical friction. Interestingly, at “ $z=1$ ” there is little difference in the evolution of the orbit between the most likely infall (REF) and the most radial one (RAD), compared to the corresponding experiments at “ $z=0$ ”. This indicates that the effect of the dynamical friction is more similar in these experiments at “ $z=1$ ”. This can be understood as a consequence of the different structure of the group DM halo at different redshifts.

In general, DM halos are found to be less concentrated at higher redshift, for a fixed virial mass. That is, its mass content is more evenly distributed with radii in halos at higher redshift. Then, in those halos, the efficiency of dynamical friction is expected to show less variation with radius, in comparison to more concentrated halos. Thus, one can also expect less differences in the orbital evolution of galaxies having different initial orbital eccentricities.

Summarising, galaxies in more eccentric orbits and/or with higher galaxy-to-group mass ratios experience stronger dynamical friction as they orbit in a group, which makes them decay faster towards the group centre. At higher redshift, galaxies with different initial eccentricities show less differences in the evolution of their orbits, at fixed halo mass. This can be linked to the less centrally concentrated mass distribution of groups at higher redshift, which causes weaker radial variations in the dynamical friction acting upon galaxies.

3.2 Mass loss

In order to quantify how much bound mass (both DM and stars) galaxies retain as they orbit within a group environment, the following algorithm was used: (i) Consider all DM and stellar particles of the galaxy that were bound at the previous snapshot as bound at the current snapshot. If the current snapshot is the initial one, then all galaxy particles are considered bound by construction; (ii) Compute the total bound mass of the galaxy and the velocity of its centre

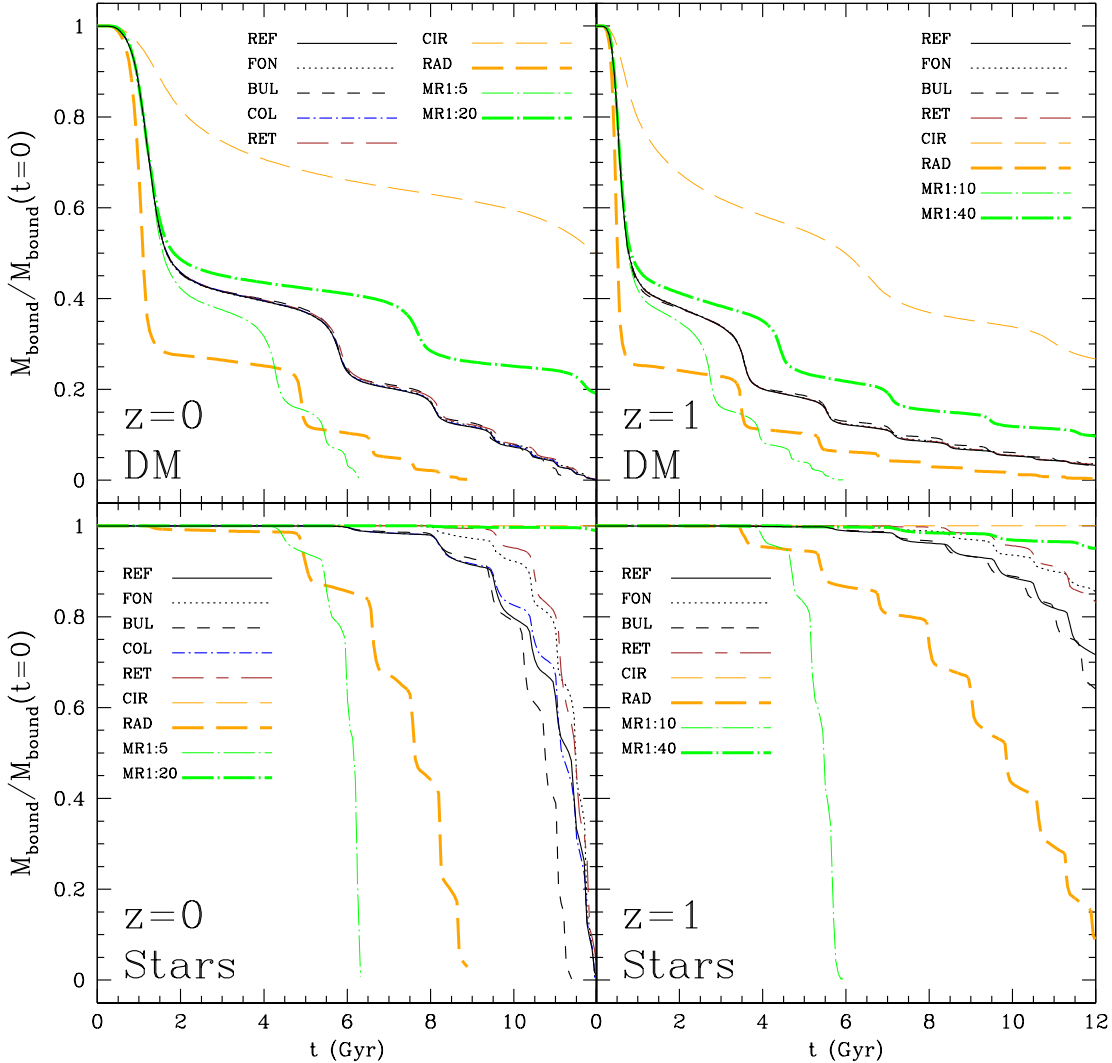


Figure 3. Evolution of the mass fraction (both DM and stars) that remains bound to the galaxy during the galaxy-group interaction, for all our experiments at redshift epochs “ $z=0$ ” and “ $z=1$ ”.

of mass; (iii) Compute the binding energy of the particles that are considered bound using the updated velocity of the galaxy’s centre of mass; (iv) Retain only those particles that are still bound (i.e., with negative binding energy), and recompute the total mass of the galaxy; (v) If the total bound mass from (ii) and (iv) has converged, then record it and go back to (i) for the next snapshot. If the total bound mass has not converged, then go back to (ii) using the bound particles found at step (iv).

Figure 3 shows the evolution of the number of particles that remain bound in both the DM halo and the stellar disc of the galaxy during its infall within the group environment. In general, the evolution is characterised by alternating phases of fast and slow mass loss rates, which are closely related to the orbital evolution of the galaxy. Phases of fast mass loss take place when the galaxy is near one of its pericentric passages, where DM particles and disc stars in the galaxy suffer significant impulsive accelerations by the

group potential. On the other hand, slow phases of mass loss occur when the galaxy approaches the apocentres. In general, galaxies lose DM mass much earlier than stellar mass. In most cases, more than half of the initial DM mass is lost after the first pericentric passage of the galaxy, while stellar discs are able to retain half of their initial mass after several pericentric passages. This can be explained by the fact that DM halos are less concentrated and (initially) more radially extended than stellar discs. As galaxies orbit within the group, the barely-bound external particles of halos are quickly removed as they encounter the high density central region of the group, where they experience strong impulsive accelerations. On the other hand, disc stars sit at the bottom of the potential well of the galaxy, where they require a significant increase in their kinetic energies to be removed from the discs, therefore remaining bound to the galaxy for longer times.

In our simulations, the extreme cases in the evolution

of mass loss are found for the experiments that explore different orbital eccentricities and galaxy-to-group mass ratios. Namely, at “ $z=0$ ”, the CIR; RAD; MR1:5 and MR1:20 experiments, and at “ $z=1$ ”, the CIR; RAD; MR1:10 and MR1:40 experiments. With respect to the REF experiment, more DM mass remains bound to the galaxy halo in the CIR; MR1:1:20 and MR1:40 experiments, that have in common the fact of being affected by less efficient dynamical friction (see §3.1), which keeps the galaxies away from the central region of the group where strong accelerations at pericentric passages are more intense. In these experiments, discs are capable to retain most of their mass (>95 per cent) over 12 Gyr of evolution within the group environment. On the other hand, in the RAD; MR1:5; and MR1:10 experiments, the dynamical friction is more efficient and galaxies are dragged towards the central region of the group early on during the infall. In these cases, both DM and stellar mass are stripped faster than in the REF experiment. Typically, DM halos only retain ~ 30 -40 per cent of their mass after the first pericentric passage, while discs can delay the start of their mass loss until the third pericentric passage.

The rest of the experiments (i.e., FON, BUL³, COL, RET) show an evolution of DM mass loss that is basically identical to that in the REF experiment. This is to be expected since those experiments explore different configurations related only to the galaxies’ discs. On the other hand, the stellar mass loss in those experiments show very interesting variations. Discs infalling with different inclinations with respect to their orbital planes (REF vs. FON vs. RET) lose stellar mass in distinct ways during the infall within the group. RET experiments (where discs have their intrinsic and orbital angular momentum vectors antiparallel) are shown to retain up to ~ 15 per cent more stellar mass along their orbits, with respect to the REF experiments (which have the aforementioned angular momentum vectors parallel)⁴. Interestingly, the FON experiments, in which discs infall face-on (i.e., their intrinsic and orbital angular momentum vectors are orthogonal), show an intermediate behaviour with respect to the REF and RET experiments, where discs infall edge-on. This suggests that the inclination of the stellar discs with respect to their orbits is an important factor for galaxy evolution during the infall within groups (see Section 3.3). Note also that, at “ $z=0$ ”, the discs in the REF, FON and RET experiments have all lost almost completely their stellar content by the end of the simulations (~ 12 Gyr), independently of differences in their past evolution. This shows that the longer the discs retain their mass during intermediate stages of the infall, the faster they will lose it at later times. This can be understood in terms of the role played by dynamical friction during the infall. The more mass a disc retains, the more efficient the influence of dynamical friction is, which brings the disc close to the centre of the group on shorter timescales. Here, it can be affected by stronger impulsive accelerations, leading to a faster mass

loss rate. In a similar vein, the presence of a central stellar bulge in the disc in the BUL experiment (with 1/3 of the disc’s mass), deepens the potential well enough to allow the disc to retain slightly more bound mass during the first part of the infall, in comparison to the REF experiment. Similarly to the FON and RET experiments, this retention of extra bound mass makes the disc in the BUL experiment to lose mass faster at later stages of the infall. This type of behaviour is seen yet again for the COL experiment, where the colder kinematics of the disc (i.e., with a lower Q parameter) keeps the stars closer to the midplane, which makes them less likely to get stripped during the early stages of the evolution. Again, the disc is able to temporarily retain more bound mass, only to lose it faster by the end of the infall, compared to the REF experiment.

Note that, in general, the fraction of bound stellar mass decreases more slowly in the experiments at “ $z=1$ ”, compared to those at “ $z=0$ ”. This can be understood as a consequence of the more compact discs at “ $z=1$ ”, and of the shallower radial variation of the global potential well, due to the less concentrated mass distribution of the group at higher redshift. This leads to weaker and less destructive impulsive accelerations affecting the disc at each pericentric passage, which helps preserving for a longer time the mass originally bound to the discs. This highlights the key role played by the structure of the environment on the evolution of disc galaxies.

Summarising, we find that galaxies with more eccentric initial orbits and those with higher galaxy-to-group mass ratios experience a faster loss of bound mass, in comparison to the reference experiment. This occurs as a consequence of the more efficient dynamical friction affecting the galaxies in the first cases, which brings them faster within the dense central region of the group, exposing them to stronger impulsive accelerations. Additionally, the initial inclination of disc galaxies, with respect to their orbital planes, is found to be an important factor in the evolution of their mass loss. In particular, galaxies with infalling inclinations of 90° and 180° are found to be able to retain increasingly more mass during intermediate stages of the orbit, compared to galaxies with 0° inclination. We also find that when galaxies retain more mass during intermediate stages of the infall, they end up losing it faster at later times. This is also related to the more efficient dynamical friction acting on more massive galaxies. Finally, less concentrated groups, in experiments at higher redshift, are found to be linked to significantly less violent decreases in the fraction of bound stellar mass of galaxies, given that they provide a relatively weaker global force field.

3.3 Disc morphology

As shown in the previous section, disc galaxies go through significant evolution in their stellar content as they orbit within a group environment.

Figures 4–7 show the evolution of the morphology of disc galaxies in the REF, FON and RET experiments at “ $z=0$ ” and “ $z=1$ ”. These experiments explore different initial inclinations of the discs with respect to their orbital planes. Changes in the morphology are illustrated in terms of (equally-spaced) number density contours, considering only

³ Throughout the paper the outcome of our BUL experiments is analysed exclusively from the point of view of the evolution of the disc. Only disc stars are included in all measurements, excluding stars belonging to the bulge by construction.

⁴ Note that our definition of retrograde infall differs from that used in Murante et al. (2010), where the sense of the orbit was defined with respect to the primary halo/disc spin.

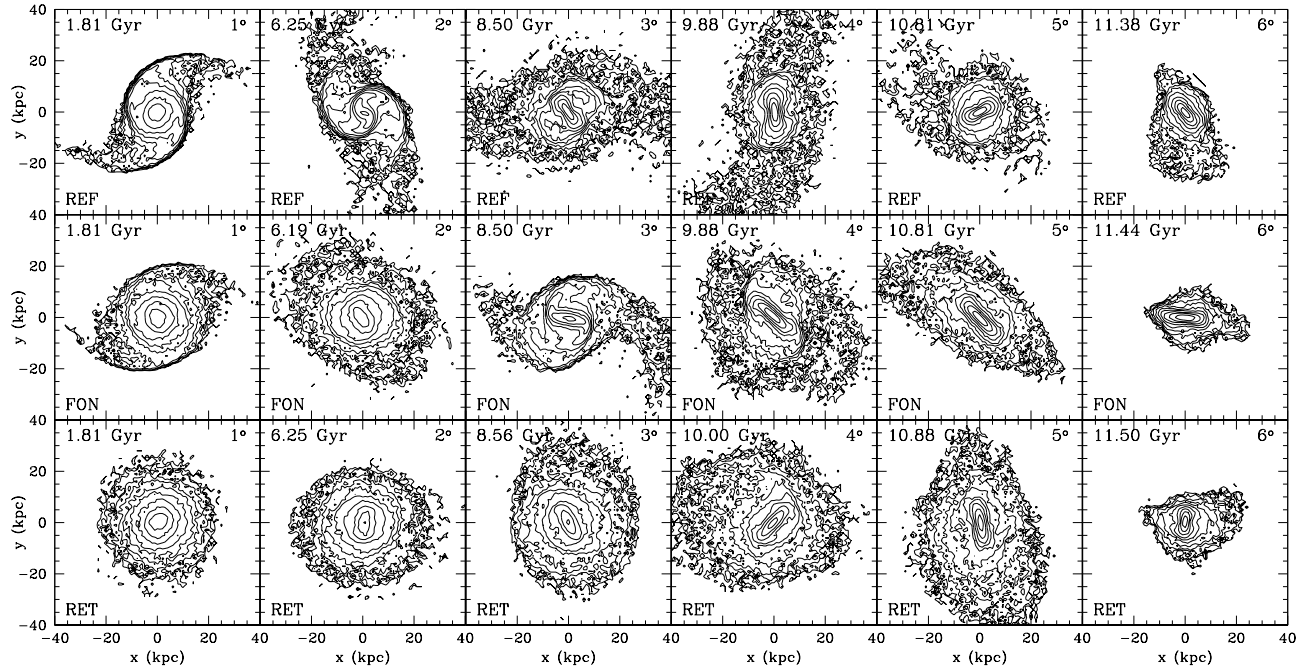


Figure 4. Face-on views of the morphological evolution of disc galaxies for our REF (reference), FON (face-on infall) and RET (retrograde infall) experiments at “ $z=0$ ”, after each of their first six pericentric passages. Number density contours are drawn at the same levels to ease the comparison, and only stars that remain bound to the disc, at a given time, are considered.

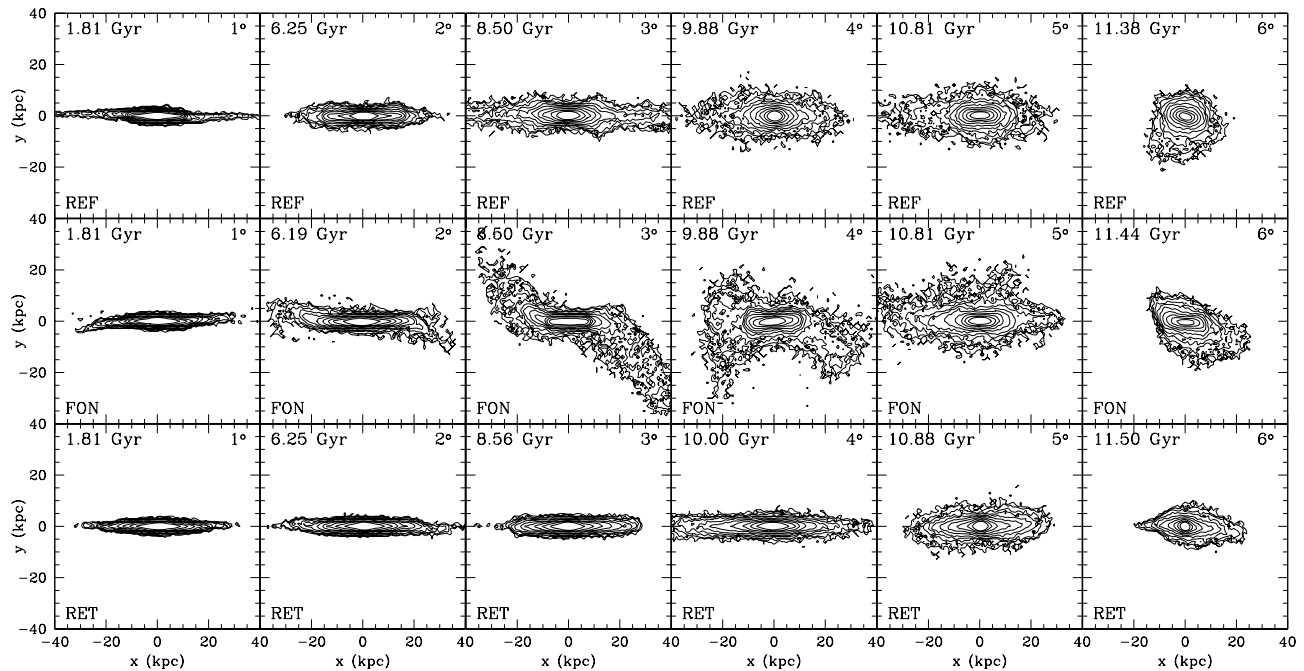


Figure 5. Same as Fig. 4 but in edge-on view.

disc stars that remain bound at the respective pericentric passage.

The Figures show striking differences in the morphology of discs after the first pericentric passage. Disc galaxies in the REF experiments are characterised by the formation of strong tidal arms, while in the RET experiments discs main-

tain their initial circular shape. Interestingly, discs in the FON experiments are an intermediate case, showing milder tidal arms than in REF, but conserving most of their initial shape, as in RET. Note that the first pericentric passage occurs after the same infall time and at the same distance from the group centre, for all three experiments at a

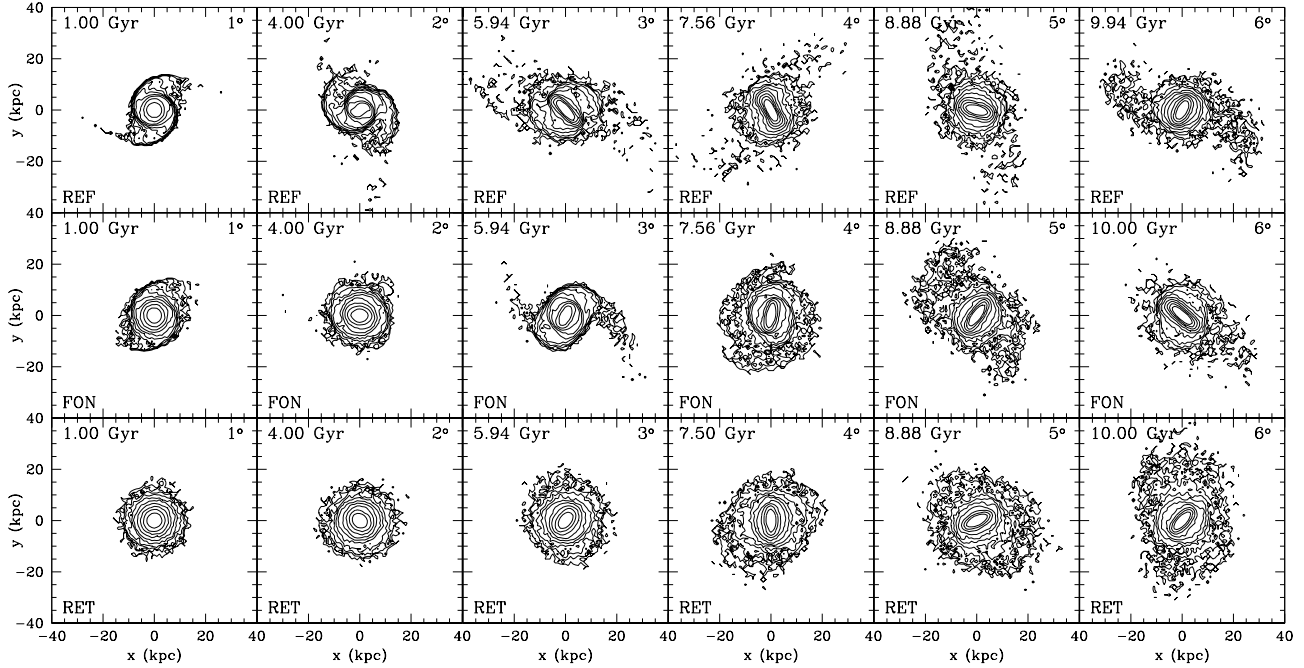


Figure 6. Face-on views of the morphological evolution of disc galaxies for our REF (reference), FON (face-on infall) and RET (retrograde infall) experiments at “ $z=1$ ”, after each of their first six pericentric passages. Number density contours are drawn at the same levels to ease the comparison, and only stars that remain bound to the disc, at a given time, are considered.

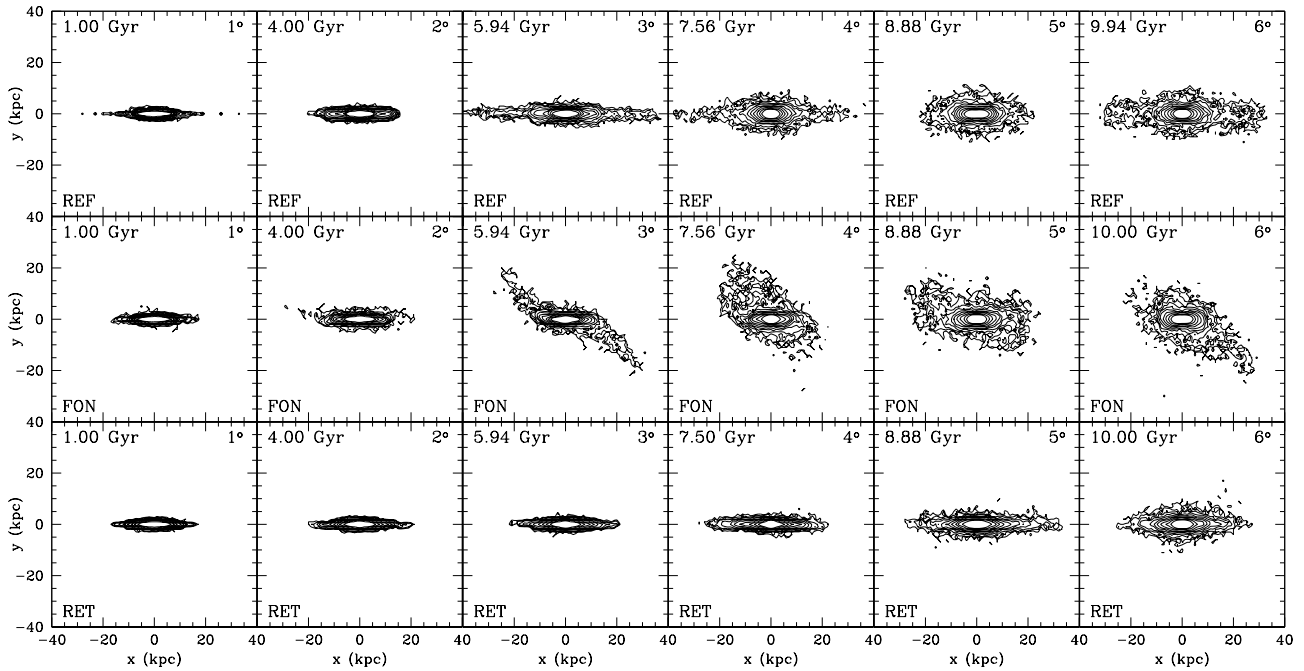


Figure 7. Same as Fig. 6 but in edge-on view.

given redshift. Therefore, all three discs are affected by the same global force. A very similar evolution is observed up to the fourth (sixth) pericentric passages at “ $z=0$ ” (“ $z=1$ ”). In general, discs in the FON and RET experiments show a remarkable increasing resilience against the formation of tidal arms, with respect to discs in the REF experiments.

The different evolution of discs in prograde and retrograde orbits, regarding the formation of tidal arms, can be explained by the different net tangential velocities of stars on opposite sides of the disc during a pericentric passage. In a prograde orbit, disc stars that are closer to the group centre have lower angular momenta than the disc centre of

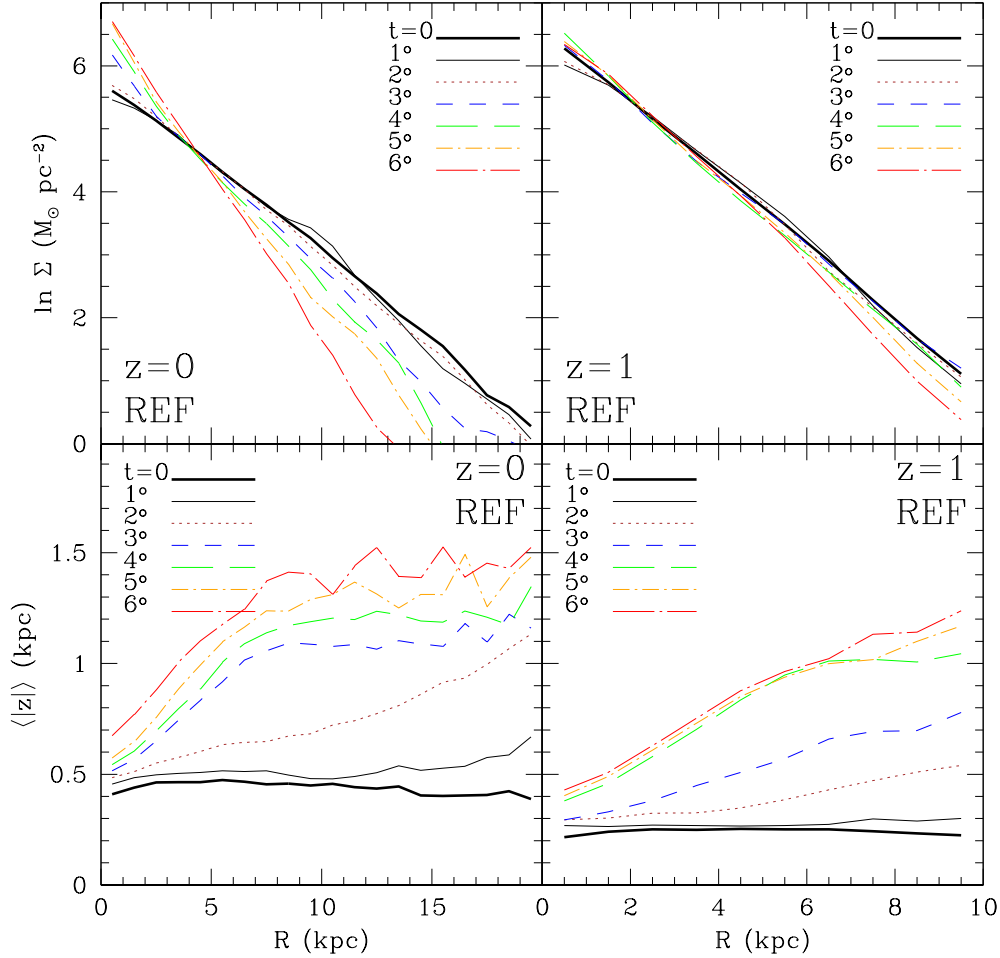


Figure 8. Evolution of the mass surface density and thickness profiles of disc galaxies, for our REF (reference) experiments at “ $z=0$ ” and “ $z=1$ ”, after each of their first six pericentric passages. The profiles have been computed in concentric rings, 1 kpc wide, considering only stars that remain bound and are located within 3 kpc from the midplane. At each radius the thickness of discs is computed as $\langle |z| \rangle$.

mass, with respect to the centre of the group, while stars on the opposite side of the disc have higher angular momenta. The combined effect of this different distribution of angular momenta and the global tidal field stretches the disc in opposite directions, inducing the formation of tidal arms. On the other hand, in a retrograde orbit, disc stars closer to the group centre have higher angular momenta than the disc centre of mass, and those on the opposite side of the disc have lower angular momenta, with respect to the group centre. In this case, the global tidal field is less efficient at stretching the disc, and the formation of tidal arms is inhibited.

Although the results discussed above are valid for disc galaxies orbiting in a group-size halo, it is interesting to note that the presence of spiral arms induced by the tidal field seems to be consistent with observations of spiral arms in unrelaxed populations of early-type dwarf galaxies in the Virgo cluster (e.g., see Lisker et al. 2007).

Figures 4–7 also show a quantitative difference in the central bars formed in each case. They appear stronger for discs in the REF experiments, and progressively milder in

the FON and RET experiments. It is interesting to notice that the relative strength of the central bars seems to correlate with the thickening generated in the discs after subsequent pericentric passages. In general, discs in the RET experiments remain significantly thinner than those in the REF experiments, while in the FON experiments the initial vertical structure of discs is considerably altered by a noticeable warping during the first pericentric passages, especially after the third one.

Finally, regarding the rest of the experiments, our simulations show that all disc galaxies on prograde orbits suffer morphological changes that are rather similar to those seen in the REF experiments. This evolution is found to be independent of the galaxy-to-group mass ratio, initial orbital parameters, presence of bulge or disc kinematics. The timescales at which these morphological changes occur, however, are directly related to the efficiency of the dynamical friction affecting the disc in each case. That is, the morphological evolution is found to be faster for galaxies with more eccentric initial orbits and/or with larger galaxy-to-group mass ratios.

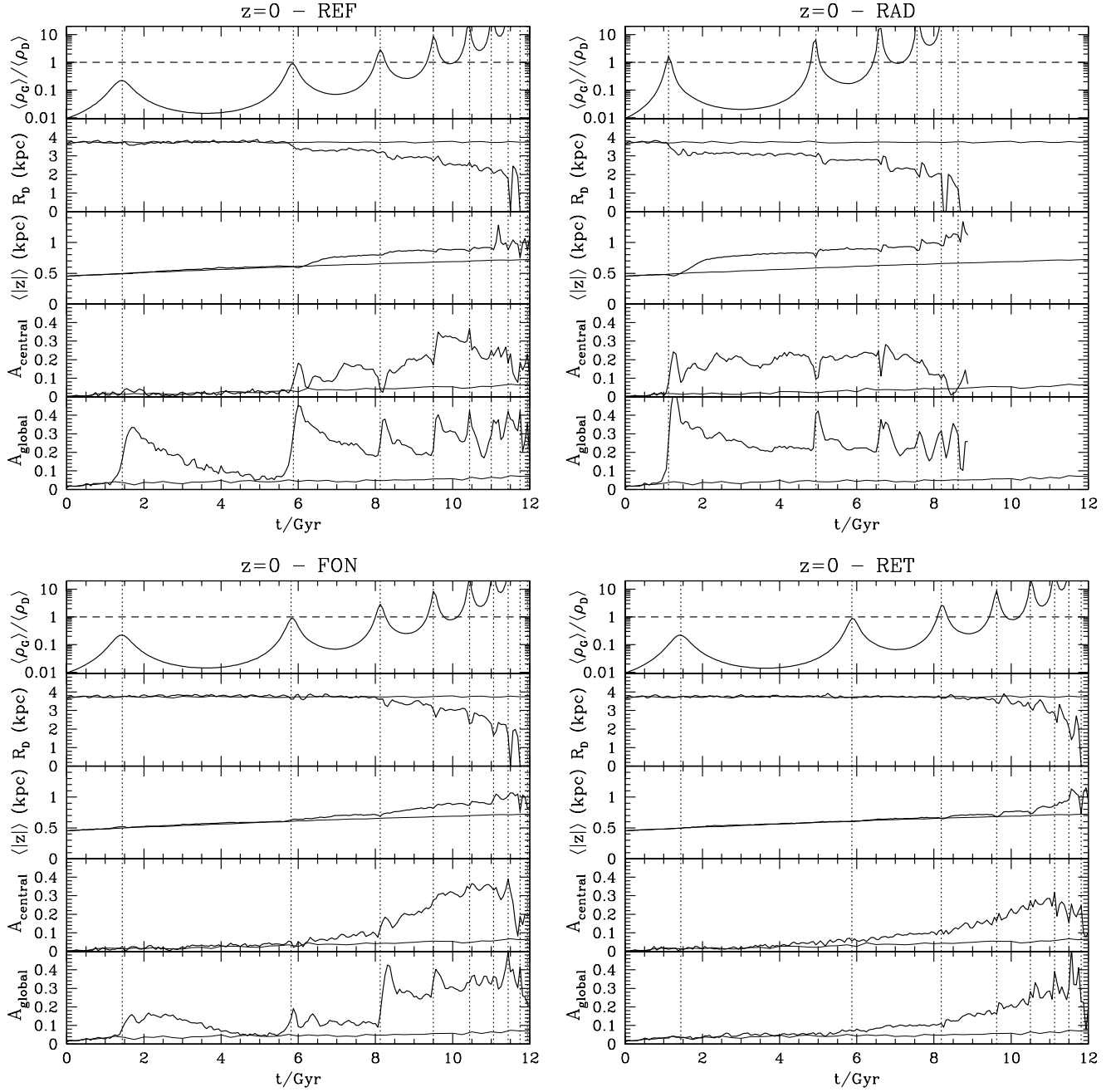


Figure 9. Evolution of the structure of disc galaxies in terms of their scale-lengths, R_D , mean thickness, $\langle |z| \rangle$, and both central and global $m=2$ Fourier amplitudes, A_{central} and A_{global} . The evolution of discs is shown along with the strength of the global tidal force acting upon them along their orbits, estimated as the group-to-galaxy mean density ratio, $\langle \rho_{\text{group}} \rangle / \langle \rho_{\text{galaxy}} \rangle$ (see details in the text). For comparison, the evolution of the structure of isolated disc galaxies (thin lines), and the times of pericentric passages (vertical dotted lines), are also included. For clarity, only the REF (reference), RAD (more eccentric infall), FON (face-on infall) and RET (retrograde infall) experiments at “ $z=0$ ” are shown, while the rest of the experiments can be found in the Appendix.

Summarising, the morphological changes experienced by disc galaxies orbiting within a group are characterised by the formation of tidal arms and a central bar, induced by the global tidal field during pericentric passages. Our simulations show that the significance of these morphological features is closely related to the initial inclination of the discs with respect to their orbital planes. The morphological evo-

lution is found to be stronger for discs with inclination 0° , and weaker for discs with inclination 180° . In the latter case, discs are able to retain their initial morphology (especially their thickness) after several pericentric passages. The morphology of disc galaxies with initial inclination 90° are typically affected by a strong warping during the first pericentric passages. All disc galaxies in prograde orbits are found to

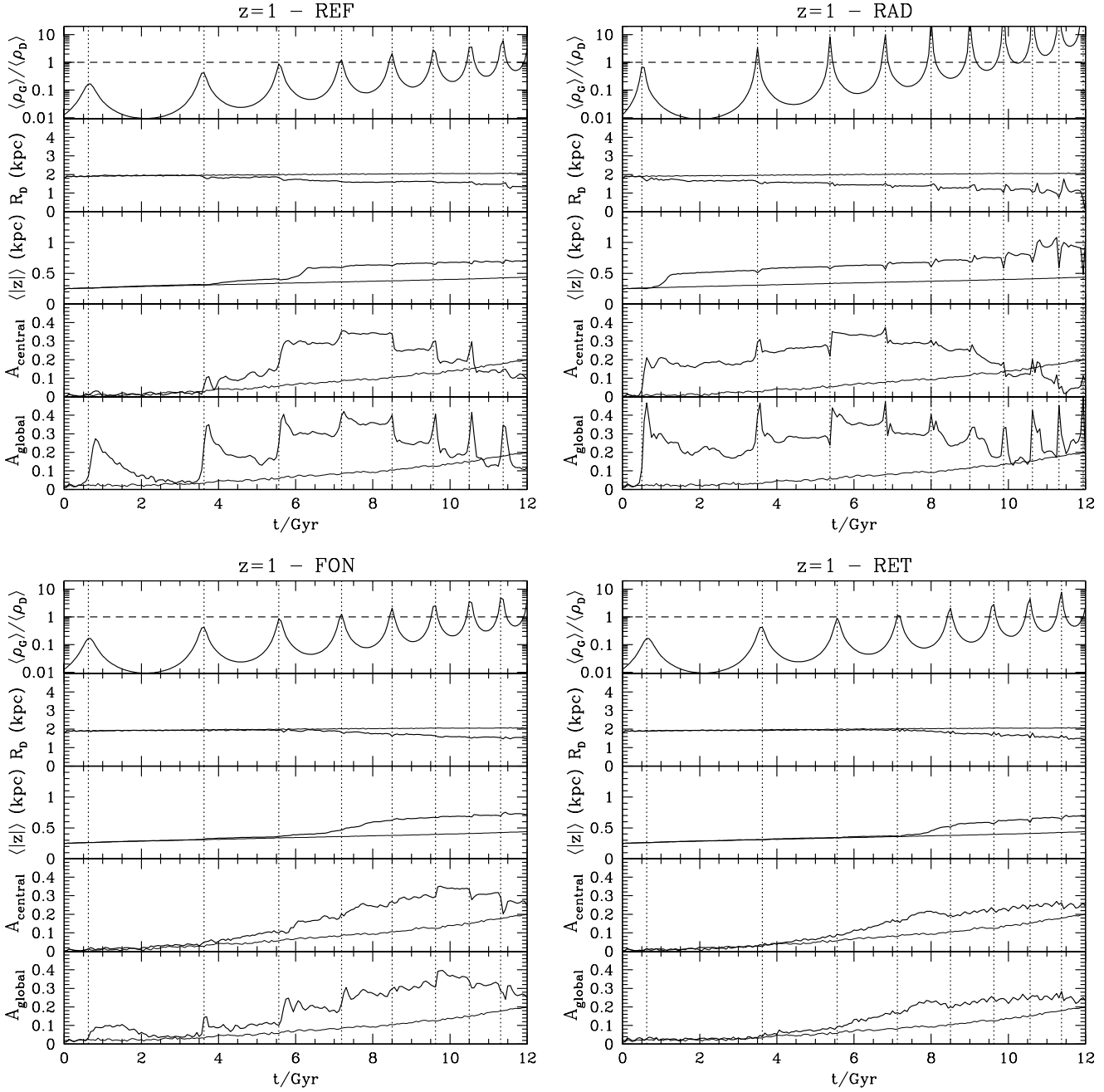


Figure 10. Same as Fig. 9, but for experiments at “ $z=1$ ”.

suffer similar morphological changes, and the timescales of these changes are directly linked to the efficiency of the dynamical friction acting on the discs.

3.4 Disc structure

In order to study the structural changes of disc galaxies, as they orbit within a group environment, we have first centred the discs and aligned them in such a way that the Z-axis is defined by their rotation axes. Then, their structural properties have been computed in concentric rings, 1 kpc wide (out to 20 kpc from the disc centre for the “ $z=0$ ” experiments,

and out to 10 kpc for the “ $z=1$ ” experiments), considering only stars that remain bound to the disc galaxy at a given time, and that are located within 3 kpc from the midplane⁵.

Figure 8 shows the evolution of the surface mass density profiles $\Sigma(R)$ of discs in the REF experiments at redshift “ $z=0$ ” and “ $z=1$ ”, after each of their first six pericentric passages. The profiles show that discs start losing stars from the outskirts first. This is expected since those stars

⁵ No significant variations in either the structural or the kinematical properties of discs are found for different (reasonable) vertical limits.

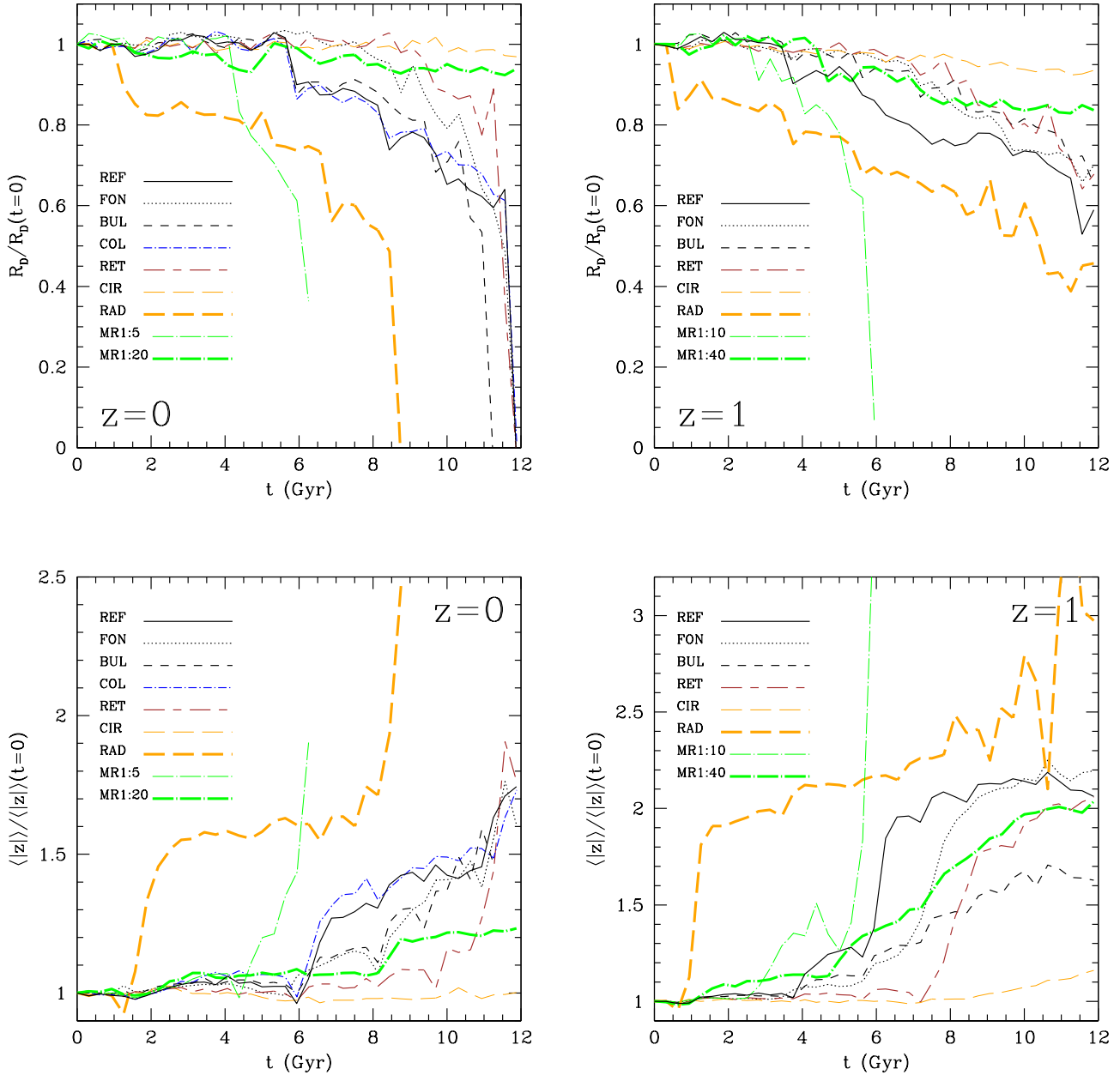


Figure 11. Evolution of the scale-lengths and the mean thickness of discs galaxies for all our experiments at redshift epochs “ $z=0$ ” and “ $z=1$ ”. Both the scale-lengths and mean thickness have been normalised by their corresponding initial values, and have been corrected by the evolution of the respective disc in isolation.

have lower binding energies and can be more easily stripped off, especially after strong tidal interactions between the disc and the central region of the group during pericentric passages. On the other hand, there is an increase of the surface mass density in the central region of the discs (most notably at “ $z=0$ ”), due to the accumulation of mass that forms a central non-axisymmetric feature. Interestingly, the surface mass density profiles stay fairly exponential (seen as a straight line in log-linear scale) during the evolution of the discs, in spite of the central feature formed at later times.

In our experiments, we have computed the scale-length of discs by applying a linear fit to $\ln \Sigma(R)$. We have considered only bound stars out to $0.75R_D$ (where R_D is the initial disc scale-length), in order to avoid spurious measurements due to tidal arms. The evolution in the radial structure of the stellar discs, during their infall within a group environment, is characterised by a steady decrease in the scale-length of their mass distributions. Note that the decrease in the surface mass density at larger radii appears more significant at “ $z=0$ ” than at “ $z=1$ ”. This is consistent with the faster mass

loss rate observed during pericentric passages at “ $z=0$ ”, as described in Section 3.2.

Figure 8 also shows the evolution in the thickness of the stellar discs as a function of radius, after each of their first six pericentric passages, for the REF experiments at redshift “ $z=0$ ” and “ $z=1$ ”. At each radius, the thickness is expressed as $\langle |z| \rangle$. As discs orbit within the group environment, they are subject to significant thickening that is not uniform with radius, but more pronounced towards the outskirts. In the REF experiments, most of the evolution in the thickening of the discs is seen before the third (fourth) pericentric passage at “ $z=0$ ” (“ $z=1$ ”). In fact, we shall see that the pericentric passage at which the first significant change in the thickening takes place is clearly correlated to the appearance of a central non-axisymmetric feature in the disc. Since the thickening increases with radius, we have adopted a single *global* thickening in order to compare discs of different experiments. This global thickening has been defined as a “mean” thickening averaged over radial bins, and weighted by the number of stars in each bin.

Interestingly, our simulated discs resemble the unrelaxed populations of early-type dwarf galaxies observed in the Virgo cluster, which have exponential brightness profiles and oblate intrinsic shapes (Lisker et al. 2007). However, as mentioned above, our simulations might not be directly comparable to those observations.

In the context of our simulations, the evolution of disc galaxies is exclusively driven by tidal interactions with the global potential of the group environment. This motivates us to examine the structural changes in the discs with respect to the strength of the global tidal forces acting upon them. Figures 9 and 10 show the evolution of the scale-length and scale-height of discs, and of the amplitudes of their central and global non-axisymmetries, comparing them to the evolution of the global tidal force on the disc galaxies along their orbits. This is shown for the following representative experiments: REF, RAD, FON and RET, at redshift epochs “ $z=0$ ” and “ $z=1$ ”. Also included are the times at which the pericentric passages take place, as well as the structural evolution of the discs in isolation (scale-length, scale-height and amplitudes of non-axisymmetries), that is, without the interaction with the group environment. The strength of the global tidal force acting on discs along their orbits is estimated as the group-to-galaxy mean density ratio, $\langle \rho_{\text{group}} \rangle / \langle \rho_{\text{galaxy}} \rangle$. Both $\langle \rho_{\text{group}} \rangle$ and $\langle \rho_{\text{galaxy}} \rangle$ are computed considering both DM and stellar mass, the former within the disc’s orbit from the centre of the group, and the latter within $10R_{\text{D}}$ from the disc centre. The amplitudes of the $m=2$ non-axisymmetries are computed by binning the spatial distribution of bound disc stars in cylindrical shells of 1 kpc width, out to $\sim 6R_{\text{D}}$. In each bin, the second harmonics of angular distribution are computed as:

$$a_2 = \frac{1}{N} \sum_{i=1}^N \sin(2\phi_i), \quad b_2 = \frac{1}{N} \sum_{i=1}^N \cos(2\phi_i), \quad (4)$$

where in each bin, N and ϕ_i are the number of stars and their angular position, respectively. The amplitude of the $m=2$ harmonic, in each bin, is $A^2 = (a_2^2 + b_2^2)/2$. We define the global amplitudes as $A_{\text{global}} = \sqrt{\langle A(R)^2 \rangle}$, averaged over radial bins, and the central amplitudes as $A_{\text{central}} = A(R)$, for stars within $R < 6R_{\text{D}}$.

Figures 9 and 10 show the very close relation between the structural evolution of the discs, and the evolution of the global tidal force acting on them along their orbits. In general, as discs orbit within the group potential well, the relative strength of the global tidal force, $\langle \rho_{\text{group}} \rangle / \langle \rho_{\text{galaxy}} \rangle$, varies along the orbit, starting from a small tidal force at the virial radius of the group, where $\langle \rho_{\text{group}} \rangle \approx 0.01 \langle \rho_{\text{galaxy}} \rangle$. As discs approach their first pericentric passage, $\langle \rho_{\text{group}} \rangle / \langle \rho_{\text{galaxy}} \rangle$ spikes because of the rapid increase in the mean density of the group within the disc’s orbit. By the time $\langle \rho_{\text{group}} \rangle \approx \langle \rho_{\text{galaxy}} \rangle$ (or in the case of experiments at “ $z=1$ ”, $\langle \rho_{\text{group}} \rangle \approx 0.3\text{--}0.5 \langle \rho_{\text{galaxy}} \rangle$), the global tidal force is strong enough to trigger significant transformations in the structure of discs. In particular for the REF experiments, the enhanced mass loss at this point (see Figure 3) leads to a sharp decrease in the scale-lengths of discs. At the same time, the formation of central non-axisymmetries (possibly triggered by the generation of tidal arms, according to the amplitude of global non-axisymmetries), heats the discs vertically, increasing their scale-heights. When $\langle \rho_{\text{group}} \rangle < \langle \rho_{\text{galaxy}} \rangle$, the global tidal force at pericentres is only able to excite the formation of global non-axisymmetries, and of negligible central non-axisymmetries. On the other hand, when $\langle \rho_{\text{group}} \rangle > \langle \rho_{\text{galaxy}} \rangle$, the discs experience a series of step-like decreases in their scale-lengths, and step-like increases in their scale-heights, at subsequent pericentric passages. These step-like changes in the structure of discs highlight the fact that most of the evolution suffered by discs takes place at the pericentres. This is expected since at those points along the orbits of discs, the impulsive accelerations on them are the strongest.

Our finding that discs start suffering significant structural transformations after $\langle \rho_{\text{group}} \rangle \gtrsim \langle \rho_{\text{galaxy}} \rangle$ agrees *only partially* with the recipe for tidal disruption used in the semi-analytic model of galaxy evolution by Guo et al. (2011). The following are some important differences between this recipe and the results of our simulations. First, this criterion is applied only after the galaxy DM halo has been completely disrupted. Our simulations show that by the time discs are affected by tidal forces, their DM halos still retain a non-negligible fraction of their initial mass. Second, their estimation of $\langle \rho_{\text{galaxy}} \rangle$ only considers baryonic material, while ours takes into account both DM and stellar mass. Lastly, Guo et al. assume that the galaxy is completely disrupted when the criterion is satisfied. Our simulations show that this recipe can underestimate significantly the disruption time of galaxies, since they can survive for a much longer time after they start being affected by the tidal forces of the global field.

The rest of the experiments at “ $z=0$ ” show a behaviour that is qualitatively similar to that of the REF experiment. The specific differences between them are, firstly, how rapidly along their orbits the discs are dragged into regions where $\langle \rho_{\text{group}} \rangle \approx \langle \rho_{\text{galaxy}} \rangle$; and secondly, how much the structure of discs responds to the strong tidal forces, based on the initial inclination of their orbits. In the RAD experiment, given that the disc has a more eccentric infalling orbit in comparison to the disc in the REF experiment, it experiences changes in its structure significantly sooner along the orbit. In particular, it reaches the central region of the group where $\langle \rho_{\text{galaxy}} \rangle \approx \langle \rho_{\text{group}} \rangle$ during its first pericentric passage. The disc in the RET experiment has a structural

evolution significantly different from that of the REF experiment, despite having a very similar infalling orbit. It shows an almost complete absence of both global and central non-axisymmetric features correlated with pericentric passages. The former can be associated to a slower mass loss rate (see Figure 3), and to a slower decrease in the disc scale-length. The latter can be linked to the formation of a weak central bar that does not increase the disc scale-height dramatically. The characteristics of the disc in the FON experiment lie in between the two extreme behaviours described for the REF and RET experiments, thus providing an intermediate case for the structural evolution of discs.

Figure 11 shows a direct comparison of the evolution of the scale-lengths and scale-heights of discs, for all the experiments at “ $z=0$ ” and “ $z=1$ ”. We find that the experiments at “ $z=0$ ” that evolve the most, in terms of scale-lengths, are RAD and MR1:5. In those cases, the initially more eccentric orbit and the larger galaxy-to-group mass ratio are linked to a more efficient dynamical friction, that drags the galaxies towards the centre of the group on shorter timescales. In these discs, the scale-lengths decrease by ~ 50 per cent right before reaching the group centre at $t \sim 6.5$ -8.5 Gyr. On the other hand, the discs that evolve the least are found in the CIR and MR1:20 experiments, in which the discs spend most of the time at the outskirts of the group, away from the denser central region. In those cases, the scale-lengths show a decrease of less than 10 per cent over 12 Gyr. The rest of the experiments show an intermediate evolution where the scale-lengths decrease by ~ 60 per cent before they reach the group centre at $t \sim 11.5$ -12 Gyr. However, some of these experiments do show some different evolution while discs are infalling. The scale-lengths in the FON and RET experiments change less over time with respect to REF experiments, which is consistent with the different ways these discs generate tidal arms and lose their bound mass. On the other hand, the scale-lengths of discs in the BUL and COL experiments show practically no differences in comparison to the REF experiment.

The evolution of the discs’ scale-lengths in the experiments at “ $z=1$ ” show some interesting differences with respect to those at “ $z=0$ ”. Discs in the RAD and MR1:10, CIR, and REF experiments still exhibit the largest, smallest and intermediate evolution in their scale-lengths, respectively. The scale-lengths in the rest of the experiments show almost no differences among them, and in general, they present less evolution in comparison to the REF experiment. This lack of differentiation between the scale-lengths of most of the experiments at “ $z=1$ ” could be due to the relatively smaller tidal disruption of the discs by a less concentrated group environment in comparison to that at “ $z=0$ ”.

In terms of disc scale-heights, the experiments at “ $z=0$ ” that present the most evolution are RAD and MR1:5, showing up to ~ 50 per cent increase by the time the discs reach the group centre. This is consistent with what is observed for the disc scale-lengths. At the opposite extreme, the CIR experiment shows almost no thickening of the disc during 12 Gyr of evolution. Similarly to the scale-length evolution, the rest of the experiments, except MR1:20, exhibit roughly the same increase in the disc scale-heights, 50-60 per cent, right before the time they reach the group centre. Before that time, these experiments do show some differences in the amount of disc thickening. Among them, the RET ex-

periment appears to be most resistant to thickening, in comparison to the REF and COL experiments, followed by discs in the FON and BUL experiments.

In the experiments at “ $z=1$ ”, the disc thickening shows more differences between the various cases, in comparison to the scale-length evolution. While the largest increase in the scale-heights are in the RAD and MR1:10 experiments, with roughly the double mean thickness by $t \sim 6$ Gyr, the CIR experiment shows no thickening over 8 Gyr of evolution. The rest of the experiments have increments in their disc scale-height of ~ 50 -100 per cent between $t \sim 8$ -12 Gyr. Note that the presence of a central bulge does reduce the amount of thickening in the disc, with respect to the REF case. Similarly, discs in the FON and the RET experiments are also found to retain their original thickness for a longer time, compared to the REF experiment.

In summary, the evolution in the radial mass distribution of discs orbiting within a group environment is characterised by a steady decline in their scale-lengths, caused by the continuous mass loss from the outskirts of the discs and the accumulation of mass in their central regions. Interestingly, the radial mass distributions of discs remain exponential, in spite of this evolution. Additionally, disc galaxies also present a significant thickening of their vertical structure. This thickening is found to take place only after the formation of a central non-axisymmetric feature in the discs. Our simulations also show a close relation between the structural evolution of discs (in terms of their scale-length, thickness, and the formation of central features), and the strength of the global tidal force acting on them. It is found that the galaxy-to-group mass ratio, the initial inclination of the discs with respect to their orbits, and their initial orbital eccentricities are among the most important factors governing the structural evolution of discs.

3.5 Disc kinematics

In order to study the kinematical evolution of stellar discs as they orbit within a group environment, we first align their rotation axes along the Z-axis of a Cartesian system centred on the disc centre of mass. Then, the disc kinematics are computed in concentric rings 1 kpc-wide, out to 20 kpc (10 kpc) in the experiments at “ $z=0$ ” (“ $z=1$ ”). We consider only stars that remain bound to the disc and that are within 3 kpc from the disc midplane. Each disc galaxy configuration has been also evolved in isolation (that is, in absence of external forces) in order to subtract the self-evolution of the discs, attempting to measure only the evolution caused by the global tidal field. The kinematical evolution of discs has been computed as follows:

$$Q^*(t) \equiv Q(t) - Q_{\text{iso}}(t) + Q(t=0), \quad (5)$$

where $Q \equiv \sigma_R, \sigma_\phi, \sigma_Z$, or $\langle V_\phi \rangle$. Namely, radial, azimuthal and vertical velocity dispersions; or mean rotational velocity.

Figures 12 and 13 show the kinematical evolution of discs after each of their first pericentric passages (up to six), for the REF, RAD, FON and RET experiments at redshift “ $z=0$ ” (“ $z=1$ ”).

The kinematic behaviour of discs is closely related to their morphological transformation. In general, the kinematical changes in discs are found to be mainly driven by the

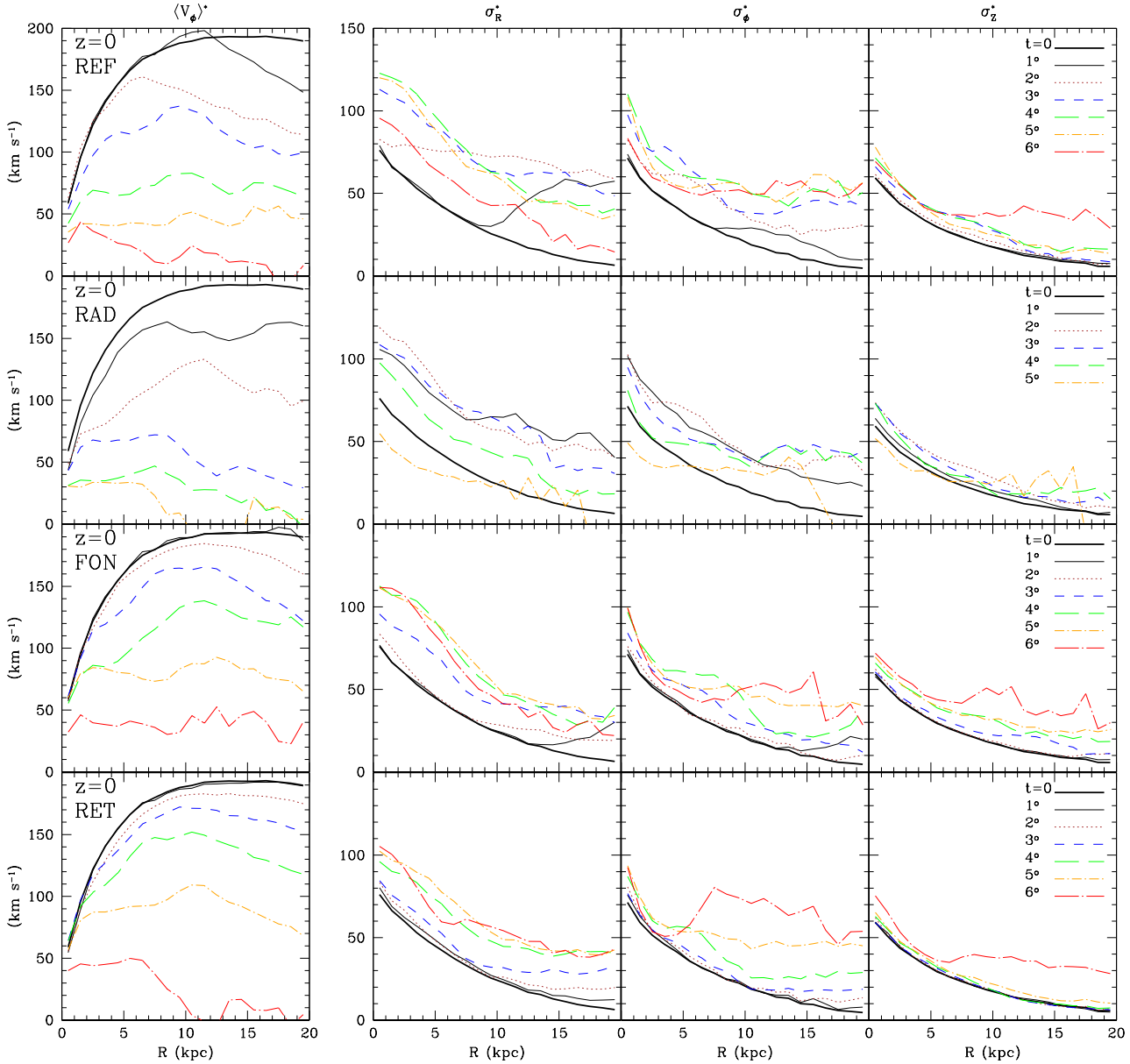


Figure 12. Evolution of the kinematics of disc galaxies in terms of their mean rotation, $\langle V_\phi \rangle$, and the radial, azimuthal and vertical components of their velocity dispersions, σ_R , σ_ϕ , and σ_z respectively, after each of their first six pericentric passages. For clarity, only the REF (reference), RAD (more eccentric infall), FON (face-on infall) and RET (retrograde infall) experiments at “ $z=0$ ” are shown, while the rest of the experiments can be found in the Appendix. The kinematics of discs have been computed in concentric rings, 1 kpc wide, considering only stars that remain bound and are located within 3 kpc from the midplane, and have been corrected by the evolution of the respective disc in isolation.

formation of tidal arms, and by the formation of central non-axisymmetric features. This, added to the step-like changes in both the discs scale-lengths and scale-heights described in Section 3.4, suggest that disc stars are typically subject to significant violent relaxation (e.g., Binney & Tremaine 1987) after each pericentric passage. The efficiency of this relaxation appears to be linked to that of the dynamical friction in each case.

In general, the REF experiments show that the kinematics of the disc is mostly affected by the formation of tidal arms during the first couple of pericentric passages,

showing a progressive increase in the coplanar velocity dispersions (both σ_R^* and σ_ϕ^*) from the outskirts of the disc inwards. Note that the formation of tidal arms does not have a significant effect on the velocity dispersions at the centre of the disc. This increment in the random motions on the plane of the disc is of course associated with a steady decrease in the ordered motion of disc stars (i.e., mean circular rotation), also from the outskirts inwards. When a central non-axisymmetric feature is formed in the disc (typically by the third pericentric passage), both σ_R^* and σ_ϕ^* increase significantly at the centre of the disc, and this increment in

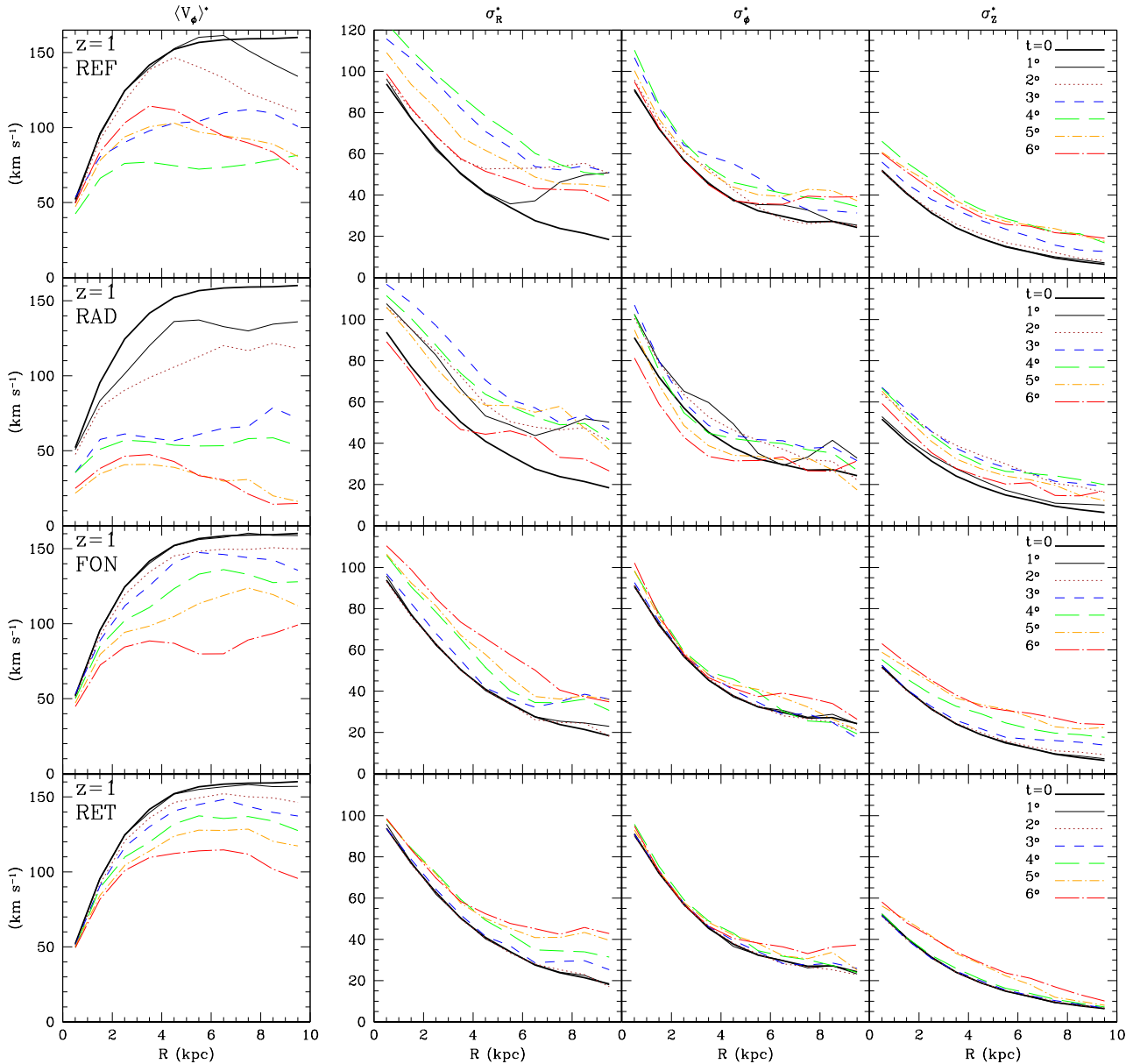


Figure 13. Same as Fig. 12, but for experiments at “ $z=1$ ”.

the velocity dispersion remains practically unchanged during the rest of the simulation. On the other hand, the mean disc rotation is observed to decrease after each pericentric passage, featuring a flat mean rotation profile as a function of galactocentric radius. In general, the vertical velocity dispersion, σ_z^* , does not show significant variations with respect to the initial profile, especially in comparison to the evolution of the velocity dispersions on the disc plane. At first sight, this might seem contradictory when confronted to the large increase in the thickness of the discs, as described in Section 3.4. According to the isothermal sheet model, $\sigma_z^2 \propto \Sigma(R)z_D$, where the terms on the right-hand side are the mass surface density of the disc and its scale-height, respectively. According to this relation, σ_z could remain roughly constant with time, if an increase in the disc

scale-height is cancelled out by a decrease in the disc surface density (see Figure 8).

In the RAD experiments, the rapid formation of central non-axisymmetric features in discs during the first pericentric passage drives the disc kinematical evolution. Therefore, we do not observe a gradual increase in both σ_R^* and σ_ϕ^* from the outskirts inwards (related to the formation of tidal arms) but instead a sudden increment at all radii, which remains roughly unchanged during several pericentric passages. In this context, the mean rotation of the disc appears to decrease faster than in the REF experiment, in subsequent pericentric passages.

Discs in the FON and RET experiments show a progressively milder kinematical evolution related to tidal arms, in comparison to the REF experiments. This is to be expected since the formation of these features is inhibited

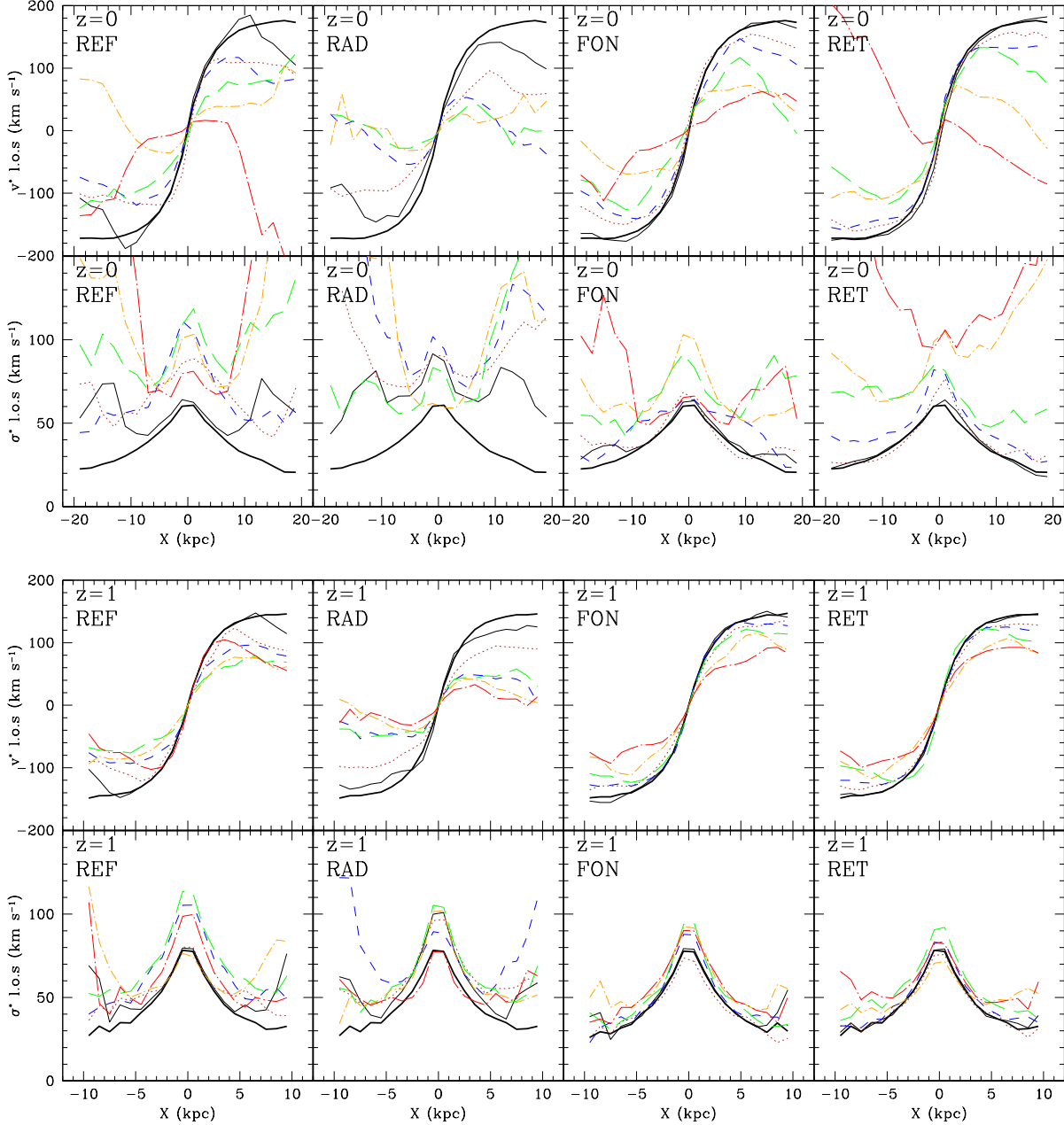


Figure 14. Evolution of the kinematics of disc galaxies in terms of their line-of-sight velocities and velocity dispersions, after each of their first six pericentric passages. For clarity, only the REF (reference), RAD (more eccentric infall), FON (face-on infall) and RET (retrograde infall) experiments at “ $z=0$ ” and “ $z=1$ ” are shown, while the rest of the experiments can be found in the Appendix. All discs are placed edge-on, with their midplanes along the X-axis. The kinematics have been computed in 1 kpc-wide bins along the X-axis, considering *all* disc stars (both bound and unbound) located within 3 kpc from the midplane, and have been corrected by the evolution of the respective disc in isolation. Both the line and colour codes are as in Figures 12 and 13.

by the initial inclination of the discs, as described in Section 3.3. Instead, in these cases the kinematical evolution of discs is mainly driven by the slow growth of the central non-axisymmetric feature, reaching a maximum increase in the velocity dispersion only after the fourth pericentric passage. This is also consistent with the fact that these discs retain for longer their initial mean rotation compared to the disc in the REF experiment.

The rest of the experiments qualitatively follow a similar kinematical evolution (see Appendix). Discs with a central stellar bulge (BUL) and that with “colder” kinematics (COL) show a kinematical evolution that is comparable to that of the REF experiments. In particular, in the BUL experiment the extra stellar mass in the central region allows the disc to retain a higher central mean rotation with respect to its outskirts, after each pericentric passage. In

the COL experiment, the early formation of a central non-axisymmetric feature appears correlated to an early increase in the coplanar velocity dispersions in the central region of the disc. Even after repeated pericentric passages, discs in more circular infalling orbits (CIR) show a negligible kinematical evolution due to the lack of interaction with the dense central region of the group. Discs in galaxies with a higher (lower) galaxy-to-group mass ratio show a rather similar evolution compared to the REF experiments. The main difference is that those discs have fewer (more) pericentric passages, with respect to the REF experiments, given the efficiency of the dynamical friction in each case.

Observationally, it is not easy to obtain three-dimensional measurements of the kinematics of disc galaxies. Let alone to distinguish between bound and unbound stars in them. Much more accessible are measurements of kinematics integrated along the line-of-sight. Similarly to Figures 12 and 13, Figure 14 shows the evolution of the kinematics of discs in our experiments at “ $z=0$ ” and “ $z=1$ ”, according to measurements of line-of-sight velocities (v_{los}) and line-of-sight velocity dispersions (σ_{los}) along their edge-on projections. In these measurements we have included *all* disc stars (i.e., both bound and unbound) with projected radii <20 kpc (<10 kpc) for our “ $z=0$ ” (“ $z=1$ ”) experiments, and within $|z|<3$ kpc⁶ from the midplane. These measurements have been corrected to account for the evolution of discs in isolation, as described above. The REF experiment at “ $z=0$ ” shows that, after successive pericentric passages, v_{los} decreases from the outskirts inwards, denoting that the disc is progressively losing rotation in the outer region. As we have seen in the previous sections, this behaviour is related to the formation of tidal arms in the external regions of the disc. After the last pericentric passage, a low remaining rotation can still be measured in the central regions of the disc, while at larger radii the disc does not exhibit ordered rotation. This is due to the presence of a small fraction of stars still bound at the centre of the disc, while the external region is mostly populated by unbound stars with higher velocity dispersions. After a the first pericentric passage, σ_{los} increases mostly at larger radii, which is consistent with the described decrease of v_{los} and the formation of tidal arms. After the following pericentric passages, σ_{los} increases significantly at smaller projected radii, which as described above is related to the formation of a central feature in the disc. At larger projected radii, σ_{los} also increases dramatically, due to the higher fraction of unbound stars with high velocity dispersions. After performing similar measurements for different (edge-on) projections of the disc, we find that measurements of v_{los} are remarkable consistent. On the other hand, σ_{los} measurements at smaller projected radii show a significant dependence on projection, given the non-axisymmetric spatial distribution of the central feature formed in the disc. At “ $z=0$ ”, the RAD experiment behaves as the REF experiment, but the disc evolves more violently, with larger decreases (increases) of v_{los} (σ_{los}) after each pericentric passage. The FON and RET experiments are also similar to the REF experiment, only being more capable of retaining larger amounts of rotation after

several pericentric passages. The REF, RAD, FON and RET experiments at “ $z=1$ ” are qualitatively similar to those at “ $z=0$ ”. However, in general, discs at “ $z=1$ ” retain more of their original rotation. The rest of the experiments (see Appendix) show similar behaviours compared to their respective REF experiments, while each of them exhibits characteristics that resemble those described in the analysis of the three-dimensional disc kinematics.

In summary, the evolution in the kinematics of discs orbiting within a group is closely linked to the morphological changes they suffer. The formation of tidal arms and of central non-axisymmetric features in the discs increases their velocity dispersions, while decreasing their rotational support. The kinematics of discs in more eccentric orbits is mostly driven by the formation of central features, since their faster orbital decay leaves less time for interactions leading to the formation of tidal arms. In a similar vein, as the formation of tidal arms is increasingly inhibited in discs with initial inclinations of 90° and 180° , their kinematical evolution is also driven by the formation of central features. Galaxies with a central bulge are able to retain a larger fraction of their rotational support, while the evolution of a disc with colder kinematics is driven early on by the formation of a central feature. Notably, galaxies in less eccentric orbits show a negligible kinematical evolution since their structures are less affected by strong global tidal forces. Differences in the galaxy-to-group mass ratios of discs are only linked to faster or slower kinematical evolution, at timescales dictated by the efficiency of the dynamical friction.

4 DISCUSSION

4.1 Comparison to similar studies

Mastropietro et al. (2005) explored the evolution of disc galaxies within a cluster environment drawn from a cosmological simulation. In their implementation, they randomly chose 20 cluster particles, replacing them with a single N -body model of a multi-component galaxy, composed by a stellar disc and a spherical DM halo. In this way, the authors simulated the evolution of discs accounting for the interaction of galaxies with the global potential, galaxy harassment by means of close encounters among galaxies (and with substructure within the cluster), as well as the hierarchical growth of the cluster as a function of redshift. Their main goal was to study the transformation of disc galaxies into dE/dSph galaxies within a cluster environment.

The experiments presented here differ from those of Mastropietro et al. in terms of the mass scale of the environment under study, the implementation of the simulations, the number of interacting galaxies, and the choice of the initial orbital parameters of galaxies. However, it is interesting to compare how galaxies evolve in the two studies, and to learn how much of the evolution of disc galaxies in a cluster environment can already be observed within a group environment.

In their study, Mastropietro et al. found that disc galaxies undergo major structural transformations, caused by both the interaction with the global cluster potential, and the close gravitational encounters with other galaxies and substructure. These structural transformations were characterised by the formation of spiral patterns and a central

⁶ Our results do not show significant differences for smaller vertical limits, down to one disc scale-height.

bar. Both tidal heating and loss of stellar mass ultimately remove the remaining spiral features, and give to the bar a rounder shape. In terms of kinematics, in spite of the loss of stellar mass, the velocity dispersion is shown to increase at the centre of the disc, driven by the formation of the bar. Nonetheless, discs are found to retain a significant amount of rotation, which helps them keep some of their original disc structure. The authors also showed that discs that orbit mostly in the outskirts of the cluster do not lose a significant fraction of their stellar mass, while they do experience structural changes, similar to those described above.

In our experiments, we observe that disc galaxies orbiting within a group-size halo show a similar evolution compared to that within a cluster environment. Namely, the discs suffer the formation of spiral patterns and of a central bar, along with increasing velocity dispersions. However, it is important to highlight some relevant differences, especially when comparing the results by Mastropietro et al. to our experiments at redshift “ $z=1$ ”. After the formation of a central bar in our discs, the tidal heating provided by the global potential is not strong enough to cause a significant mass loss that would transform the structure of the galaxies from discs to spheroidals. In our experiments, galaxies do show a significant amount of thickening, likely related to the vertical heating caused by the formation of the central bar. However, we find that the formation of a strong bar, that heats efficiently the vertical structure of the disc, is not a generic feature of the interaction between a galaxy and a group environment. Instead, it appears to depend strongly on the inclination of the disc galaxy with respect to its orbit, at the time of infall. Additionally, we observe that global changes in the structure and kinematics of discs appear to be closely correlated to the pericentric passages experienced by the galaxies during their evolution, in contrast with findings by Mastropietro et al.. Finally, we find that galaxies orbiting mostly in the outskirts of a group show a negligible loss of stellar mass, like similar galaxies evolving within a cluster. However, contrary to Mastropietro et al., we find insignificant evolution in both the structure and kinematics of those discs. Our results suggest that the group environment can indeed contribute to “pre-process” galaxies before they are accreted on a cluster. The “pre-processing” appears mild for galaxies sitting at the outskirts of groups. We stress, however, that our relatively simple experiments do not account for close encounters between group members, which could play an important role in the evolution of disc galaxies.

Note that since Mastropietro et al. assigned to their galaxies on random initial orbits, it is not straightforward to compare their results to ours, especially regarding what kind of galaxy evolution would be more likely. In addition, since their experiments included the joint effect of global tidal forces and harassment, it is not possible to isolate their separate contributions to galaxy evolution.

In a recent study, Kazantzidis et al. (2011) examined the formation of dwarf spheroidal galaxies as the result of tidal transformations in rotationally-supported disc dwarfs that interact with a MW-like galaxy. Such interactions were modelled using N -body simulations, starting from self-consistent models of stellar discs embedded in cosmologically motivated DM halos. The authors studied a broad set of configurations for the interactions, and their impact on the structure and kinematics of the final dwarf galaxies. Even

though their study is conceptually different from ours, and from that by Mastropietro et al., we consider instructive to draw parallels between disc galaxy evolution across environments of different mass scales.

Kazantzidis et al. found that dramatic tidal transformations in dwarf disc galaxies were mainly driven by efficient tidally-induced bar instabilities, as well as by strong impulsive tidal heating, taking place during pericentric passages. These mechanisms ultimately lead to the transformation of rotationally-supported discs into pressure-supported spheroids. Our results, as well as those found by Mastropietro et al. and Kazantzidis et al. confirm that disc galaxies follow a rather similar evolutionary path, where tidal transformations play a central role, independently of the masses of galaxies and the general characteristics of their respective environments. This is a consequence of the current cosmological paradigm, where encounters between structures, on rather eccentric orbits, are of common occurrence.

It is interesting to observe that, contrary to our results, Kazantzidis et al. did not find a significant variation in the evolution of dwarf discs with respect to the inclination of their infalling orbits. This is likely due to the fact that they only studied the evolution of disc galaxies on prograde orbits, with inclinations in the range $0^\circ \leq \theta \leq 90^\circ$. As described in previous sections, we find that disc galaxies infalling either face-on ($\theta = 90^\circ$) or on an edge-on retrograde orbit ($\theta = 180^\circ$) are increasingly capable of retaining stars during the infall (see also Read et al. 2006), and are increasingly resilient against the formation of a strong central bar (see also Mayer et al. 2001a). The reduced bar-driven evolution in the discs allows them to maintain their disc structure for longer times during their interaction with the global potential. This result might have potentially relevant implications for the morphology-density relation, since it would naturally account for a significant fraction of disc galaxies in the inner dense regions of groups. Indeed, prograde and retrograde infalls should be equally likely to occur. In the context of our experiments, it remains to be seen if such characteristics of discs in retrograde orbits remain in place after the addition of close-encounter interactions in our models.

Close encounters between galaxies are expected to be frequent in groups, given the number of group members in environments of this mass scale. Yang et al. (2009) have estimated the number of satellite galaxies as up to ~ 10 in groups of $\sim 10^{13} M_\odot$, using a large catalogue of galaxy groups in the redshift range $0.01 < z < 0.2$, compiled from the Sloan Digital Sky Survey Data Release 4 (Adelman-McCarthy et al. 2006). Given the velocity dispersions of groups, these encounters are low-velocity interactions, as opposed to high-velocity interactions typical of larger environments, known as harassment (e.g., Moore et al. 1998). Low-velocity close encounters would cause less impulsive but longer lasting asymmetric perturbations in the gravitational field surrounding a galaxy. The cumulative effect of these frequent perturbations are expected to play an important role in galaxy evolution, since they can induce the formation of strong tidal arms and central asymmetric features in discs, as well as, episodes of star formation. As mentioned in the Introduction, we do not include the effect of close encounters in this study. However, in the

context of our experiments, we expect that these interactions would lead to a more significant morphological evolution in disc galaxies, inducing the formation of additional tidal arms that are not correlated to the pericentric passages of galaxies. This could cause earlier formation of (possibly stronger) central asymmetric features, an even larger increase in the velocity dispersion of discs, and an accelerated rate of mass loss. We defer to a future paper of this series a detailed study of the effect of close encounters in galaxy groups, and of its relative importance with respect to the interactions with the global potential.

4.2 On the formation of S0 galaxies in groups

Galaxies classified as S0 are characterised by having little gas content, practically no signs of spiral arms, and often a prominent central bulge. Their formation process is currently unknown, although observational evidence suggests that S0 galaxies are formed from disc galaxies that experience structural, kinematical and chemical transformations, mostly induced by their environments (e.g., Dressler 1980; van Dokkum et al. 1998). It is during those transformations that their central bulges should grow significantly, in comparison to those of spiral galaxies. In recent years, there has been mounting observational evidence suggesting that group environments are more efficient at forming S0 galaxies in comparison to cluster environments (Wilman et al. 2009; Just et al. 2010). Our simulations show that the mass surface density profiles of disc galaxies remain exponential out to $\sim 6R_D$, during the evolution within a group (see Figure 8). At face-value, this result could have relevant implications for the formation of S0 galaxies in groups. Our simulations show that disc galaxies neither form central stellar bulges nor enhance pre-existing ones, during their interaction with the global tidal field. This implies that if S0 galaxies were formed within galaxy groups, then their bulges could not be produced by the effect of group tidal forces alone (e.g., via bar instabilities) on old disc stars that were already in place when the galaxy was accreted by the group. Thus, if S0 galaxies are mostly formed in groups, our simulations would support formation models in which their bulges are currently composed by a significant majority of relatively young stars (e.g., see Bekki & Couch 2011). Note, however, that our experiment exploring a lower value of the galaxy Q parameter (COL experiment) does show a relatively small accumulation of stars in the central region of discs, compared to the reference experiment. This behaviour is expected since discs that are kinematically colder (i.e., have lower Q parameter) are less resilient against the formation of central non-axisymmetries. A detailed analysis of the dependency of the size of the central non-axisymmetric features as a function of the Q parameter of disc galaxies is, however, beyond the scope of this paper.

4.3 On models of tidal disruption/stripping

All recent semi-analytic models of galaxy formation (SAMs) exhibit an excess of faint and passive satellites with respect to observational measurements (see e.g., Wang et al. 2007; Fontanot et al. 2009). In a recent paper, Weinmann et al. (2011a) have shown that the semi-analytic models pre-

dict a higher ratio of dwarf-to-giant galaxies within clusters compared to observations. In addition, they also show that SAMs do not exhibit a decrease in the dwarf-to-giant ratio, as observed in the central regions of clusters (e.g., Sánchez-Janssen et al. 2008; Barkhouse et al. 2009). Weinmann et al. argue that the most likely solution to this problem is the adoption of a more efficient tidal disruption for faint galaxies, particularly at the centre of clusters.

Diemand et al. (2004) analysed a statistical sample of dark matter substructures in a set of simulated clusters, and ascribed the lack of ‘slow’ subhalos to the fact that tidal stripping and tidal disruption is very efficient for these systems. In this scenario, faint galaxies that are also slow would be disrupted more easily by the strong tidal field of the dense central regions of clusters. In addition, faint galaxies are also less dense and have a shallower potential well, so that they are less resilient to the influence of the tidal field of the parent halo. Such a mechanism would certainly lower the overall dwarf-to-giant ratio within a cluster, especially at its centre where the tidal field is stronger. It would also explain the more extended spatial distribution of dwarf galaxies observed in clusters, as well as their broader velocity distributions. Our simulations, however, do not support this interpretation. Figure 3 shows that galaxy disruption has a much stronger dependency on both the mass ratio between the systems and on the orbital eccentricity of the infalling orbit, than on the orbital energy of the galaxy. Note that our disc galaxies in both the CIR and RAD experiments initially have practically the same orbital energy (see Table 3), however, they are disrupted in significantly different ways. Thus, our simulations offer indirect support to alternative explanations for the lower central concentration of dwarf galaxies and their higher velocity dispersion in clusters. Namely, either observed dwarf galaxies are actually an infalling population mostly located in the outer regions of cluster/groups (e.g., Conselice et al. 2001), or their characteristic radial distribution within a group/cluster is a natural consequence of energy equipartition (e.g., White 1976).

On a related subject, as pointed out by Weinmann et al. (2011a), currently there are contradictory implementations in SAMs for the tidal stripping suffered by galaxies in clusters. On the one hand, it is modelled as proportional to M/m (e.g., Kim et al. 2009), where M is the mass of the primary system and m is that of the galaxy. Even though there is not a detailed physical mechanism behind this scaling, usually it is based on the assumption that stars in smaller galaxies can be more easily stripped, since these galaxies have smaller tidal radii. On the other hand, in other studies the efficiency of tidal stripping is modelled as proportional to m/M (Wetzel & White 2010). This scaling is based on the assumption that dynamical friction is more efficient for larger galaxies, causing them to reach more rapidly the inner regions of a cluster/group where tidal disruption/stripping is more intense. According to our simulations (compare MR1:20 vs. REF vs. MR1:5 in Figure 3), implementations of tidal stripping scaling as m/M , i.e. more efficient for larger infalling galaxies, offer a better description of the evolution of galaxies within a group.

5 CONCLUSIONS

In this work, we studied the evolution of disc galaxies orbiting within a group-size system, using N -body simulations. We focus specifically on the changes induced by global tidal forces on the infalling galaxies. Both the group and the disc galaxies are modelled as “live” multi-component systems, composed by both a DM halo and a stellar component. The stellar component embedded in the group, that accounts for its central galaxy, is modelled with a spherical mass distribution. The stellar disc of galaxies follows an exponential density profile. Our strategy is to examine the evolution of a single galaxy at a time, in order to isolate the effect of the global tidal forces on the disc, avoiding that of close encounters with other galaxies. The galaxy is released on an infalling orbit from the virial radius of the group, and sinks towards the inner region of the group under the effect the dynamical friction. This set-up is repeated to probe an ample parameter space that covers a number of relevant aspects of the galaxy-group interaction. Specifically, we study the different outcomes obtained from: prograde and retrograde infalls (with respect to the disc rotation), different orbital eccentricities (consistent with distributions of orbital parameters from cosmological studies), different disc inclinations, the presence of a central stellar bulge in the disc, different internal kinematics of discs, and finally, different galaxy-to-group mass ratios. For each of these aspects, our simulations are ran at two redshift epochs, “ $z=0$ ” and “ $z=1$ ”. At “ $z=0$ ”, our fiducial disc galaxy resembles a bulge-less, slightly less massive Milky Way.

Our results can be summarised as follows:

- Our simulations confirm that the evolution of disc galaxies due to a group-size tidal field is consistent with the evolution observed in previous studies across different environment mass scales (clusters and Milky Way-like environments). The general evolution of disc galaxies is characterised by the formation of tidal arms and of central non-axisymmetric features. This consistency across different environment mass scales is a natural consequence of the current cosmological paradigm, where interactions between structures along eccentric orbits are common.

- We address the question of when, along their orbits, disc galaxies start presenting significant structural transformations due to the group tidal field. Our simulations show that they take place not before the mean density of the group, within the orbit of the galaxy, is ~ 0.3 – 1 times the central mean density of the galaxies. We find that this agrees only partially with recipes of tidal disruption currently used in some semi-analytic models of galaxy evolution.

- We find that all disc galaxies on prograde orbits (i.e. where a disc rotates in the same sense as its infalling orbit) show a very similar morphological evolution. This is found to be independent of the initial orbital parameters of discs, initial galaxy-to-group mass ratio, presence of a central bulge, and internal disc kinematics. We also find that the only significant difference among these experiments is the timescale at which the morphological changes take place. This is essentially connected to how efficient the dynamical friction affecting the galaxies is in each experiment. For instance, a more efficient dynamical friction and a faster evolution in discs are observed in experiments with larger galaxy-to-group mass ratios and more eccentric orbits.

- Our simulations show that both the morphological and structural evolution of discs are strongly dependent on the initial inclination of discs with respect to their orbits. For instance, discs infalling face-on (i.e. with their midplanes perpendicular to the orbital plane) and on retrograde orbits (i.e. discs rotating contrary to the sense of their orbits), are found to be increasingly resilient against the formation of tidal arms and of strong central non-axisymmetries, with respect to discs in prograde orbits. This makes both face-on and retrograde discs more capable to retain their original disc structure and kinematics for longer times. This would explain naturally the presence of a possibly significant fraction of disc galaxies in the inner region of groups (and maybe clusters). However, such resilience of discs could be altered by the effect of close encounters with other galaxies, which are not included in this study.

- The evolution in the structure of the disc galaxies during their infall is characterised by a steady decrease in the scale-length of their mass distributions, and by significant vertical thickening, that is more pronounced towards the outskirts of discs. Faster variations in the structure of discs are observed during pericentric passages, where discs are affected the most by strong tidal impulses from the group potential. The kinematical evolution of discs appears closely related to both the morphological and structural changes they suffer. In general, it is mainly driven by the formation of tidal arms and non-axisymmetric central features, that typically increase the velocity dispersions in the discs from the outskirts inwards. Disc galaxies evolve towards being less rotationally-supported systems, with hotter (although not significantly flatter) velocity dispersion profiles.

- Discs evolving within a group tidal field neither form significant central bulges, nor enhance the pre-existing ones. Then, under the assumption that most S0 galaxies (which often have larger bulges than found in spiral galaxies) are formed in group environments, these cannot be formed by the effect of the global tidal field on “old” stars originally in the discs. Instead, our simulations would favour formation models of S0 galaxies where their central bulges are composed by a significant fraction of young stars (i.e. formed after the accretion of a galaxy onto a group).

- Our simulations do not support the concept that tidal disruption of galaxies depends mostly on their orbital energy. Such premise has been proposed in the literature to invoke a more efficient tidal disruption of slow, faint galaxies in semi-analytic models of galaxy evolution. This being aimed to improve the agreement with observations of the dwarf-to-giant ratio of galaxies in clusters, as well as its radial distribution. Our results show instead a stronger dependency of tidal disruption on both the galaxy-to-group mass ratio and the initial orbital eccentricity of discs.

- Finally, our results contradict some of the current models of tidal stripping of galaxies in clusters, used in semi-analytic models, where tidal stripping is more efficient for less massive galaxies.

The present work can be expanded along several lines, in order to improve our knowledge on how group-scale environments shape the main properties of disc galaxies. For instance, the addition of gas components to disc galaxies would allow the study of more complex physical processes, such as, strangulation and ram-pressure. In a future study

we plan to also include the effect of close encounters on the evolution of disc galaxies, aiming to quantify the relative importance of such encounters against the effect of the global tidal field.

ACKNOWLEDGEMENTS

We thank A. Biviano, F. Fontanot, A. Macciò, S. Weinmann, and D. Wilman for useful discussions and suggestions. ÁV and GDL acknowledge financial support from the European Research Council under the European Community’s Seventh Framework Programme (FP7/2007-2013)/ERC grant agreement n. 202781. This work has been partially supported by the PRIN-INAF 2009 Grant “Towards an Italian Network for Computational Cosmology”, by the European Commission’s Framework Programme 7, through the Marie Curie Initial Training Network CosmoComp (PITN-GA-2009-238356), and by the PD51 INFN Grant. The simulations were carried out at the “Centro Interuniversitario del Nord-Est per il Calcolo Elettronico” (CINECA, Bologna), with CPU time assigned under INAF/CINECA and ISCRA-B grants.

REFERENCES

- Adelman-McCarthy J. K., Agüeros M. A., Allam S. S., Anderson K. S. J., Anderson S. F., Annis J., Bahcall N. A., Baldry I. K., Barentine J. C., Berlind A., Bernardi M., Blanton M. R., Boroski W. N., Brewington H. J., Brinchmann J., Brinkmann J., Brunner R. J., Budavári T., Carey L. N., Carr M. A., Castander F. J., Connolly A. J., Csabai I., Czarapata P. C., Dalcanton J. J., Doi M., Dong F., Eisenstein D. J., Evans M. L., Fan X., Finkbeiner D. P., Friedman S. D., Frieman J. A., Fukugita M., Gillette B., Glazebrook K., Gray J., Grebel E. K., Gunn J. E., Gurbani V. K., de Haas E., Hall P. B., Harris F. H., Harvanek M., Hawley S. L., Hayes J., Hendry J. S., Hennessy G. S., Hindsley R. B., Hirata C. M., Hogan C. J., Hogg D. W., Holmgren D. J., Holtzman J. A., Ichikawa S.-i., Ivezić Ž., Jester S., Johnston D. E., Jorgensen A. M., Jurić M., Kent S. M., Kleinman S. J., Knapp G. R., Kniazev A. Y., Kron R. G., Krzesinski J., Kuropatkin N., Lamb D. Q., Lampeitl H., Lee B. C., Leger R. F., Lin H., Long D. C., Loveday J., Lupton R. H., Margon B., Martínez-Delgado D., Mandelbaum R., Matsubara T., McGehee P. M., McKay T. A., Meiksin A., Munn J. A., Nakajima R., Nash T., Neilsen Jr. E. H., Newberg H. J., Newman P. R., Nichol R. C., Nicinski T., Nieto-Santisteban M., Nitta A., O’Mullane W., Okamura S., Owen R., Padmanabhan N., Pauls G., Peoples Jr. J., Pier J. R., Pope A. C., Pourbaix D., Quinn T. R., Richards G. T., Richmond M. W., Rockosi C. M., Schlegel D. J., Schneider D. P., Schroeder J., Scranton R., Seljak U., Sheldon E., Shimasaku K., Smith J. A., Smolčić V., Snedden S. A., Stoughton C., Strauss M. A., SubbaRao M., Szalay A. S., Szapudi I., Szokoly P., Tegmark M., Thakar A. R., Tucker D. L., Uomoto A., Vanden Berk D. E., Vandenberg J., Vogeley M. S., Voges W., Vogt N. P., Walkowicz L. M., Weinberg D.H., West A. A., White S. D. M., Xu Y., Yanny B., Yocum D. R., York D. G., Zehavi I., Zibetti S., Zucker D. B., 2006, *ApJS*, 162, 38
- Balogh M. L., Baldry I. K., Nichol R., Miller C., Bower R., Glazebrook K., 2004, *ApJ*, 615, L101
- Barkhouse W. A., Yee H. K. C., López-Cruz O., 2009, *ApJ*, 703, 2024
- Bekki K., Couch W. J., 2011, *MNRAS*, 415, 1783
- Benson A. J., 2005, *MNRAS*, 358, 551
- Berrier J. C., Stewart K. R., Bullock J. S., Purcell C. W., Barton E. J., Wechsler R. H., 2009, *ApJ*, 690, 1292
- Binney J., Tremaine S., 1987, *Galactic dynamics*, Binney, J. & Tremaine, S., ed.
- Conselice C. J., Gallagher III J. S., Wyse R. F. G., 2001, *ApJ*, 559, 791
- De Lucia G., Weinmann S., Poggianti B., Aragon-Salamanca A., Zaritsky D., 2011, *ArXiv e-prints*
- Diemand J., Moore B., Stadel J., 2004, *MNRAS*, 352, 535
- Dressler A., 1980, *ApJ*, 236, 351
- Dressler A., Oemler Jr. A., Couch W. J., Smail I., Ellis R. S., Barger A., Butcher H., Poggianti B. M., Sharples R. M., 1997, *ApJ*, 490, 577
- Fontanot F., De Lucia G., Monaco P., Somerville R. S., Santini P., 2009, *MNRAS*, 397, 1776
- Gnedin O. Y., 2003, *ApJ*, 589, 752
- Gómez P. L., Nichol R. C., Miller C. J., Balogh M. L., Goto T., Zabludoff A. I., Romer A. K., Bernardi M., Sheth R., Hopkins A. M., Castander F. J., Connolly A. J., Schneider D. P., Brinkmann J., Lamb D. Q., SubbaRao M., York D. G., 2003, *ApJ*, 584, 210
- Guo Q., White S., Boylan-Kolchin M., De Lucia G., Kauffmann G., Lemson G., Li C., Springel V., Weinmann S., 2011, *MNRAS*, 413, 101
- Hernquist L., 1990, *ApJ*, 356, 359
- Just D. W., Zaritsky D., Sand D. J., Desai V., Rudnick G., 2010, *ApJ*, 711, 192
- Kazantzidis S., Lokas E. L., Callegari S., Mayer L., Moustakas L. A., 2011, *ApJ*, 726, 98
- Kim H.-S., Baugh C. M., Cole S., Frenk C. S., Benson A. J., 2009, *MNRAS*, 400, 1527
- Klimentowski J., Lokas E. L., Kazantzidis S., Mayer L., Mamon G. A., 2009, *MNRAS*, 397, 2015
- Lacey C., Cole S., 1994, *MNRAS*, 271, 676
- Lewis I., Balogh M., De Propriis R., Couch W., Bower R., Offer A., Bland-Hawthorn J., Baldry I. K., Baugh C., Bridges T., Cannon R., Cole S., Colless M., Collins C., Cross N., Dalton G., Driver S. P., Efstathiou G., Ellis R. S., Frenk C. S., Glazebrook K., Hawkins E., Jackson C., Lahav O., Lumsden S., Maddox S., Madgwick D., Norberg P., Peacock J. A., Percival W., Peterson B. A., Sutherland W., Taylor K., 2002, *MNRAS*, 334, 673
- Lisker T., Grebel E. K., Binggeli B., Glatt K., 2007, *ApJ*, 660, 1186
- Marcolini A., Brighenti F., D’Ercole A., 2003, *MNRAS*, 345, 1329
- Mastropietro C., Moore B., Mayer L., Debattista V. P., Piffaretti R., Stadel J., 2005, *MNRAS*, 364, 607
- Mayer L., Governato F., Colpi M., Moore B., Quinn T., Wadsley J., Stadel J., Lake G., 2001a, *ApJ*, 559, 754
- , 2001b, *ApJ*, 547, L123
- McGee S. L., Balogh M. L., Bower R. G., Font A. S., McCarthy I. G., 2009, *MNRAS*, 400, 937
- McGee S. L., Balogh M. L., Henderson R. D. E., Wilman

- D. J., Bower R. G., Mulchaey J. S., Oemler Jr. A., 2008, MNRAS, 387, 1605
- Mo H. J., Mao S., White S. D. M., 1998, MNRAS, 295, 319
- Moore B., Lake G., Katz N., 1998, ApJ, 495, 139
- Moore B., Lake G., Quinn T., Stadel J., 1999, MNRAS, 304, 465
- Murante G., Poglio E., Curir A., Villalobos A., 2010, ApJ, 716, L115
- Navarro J. F., Frenk C. S., White S. D. M., 1997, ApJ, 490, 493
- Quilis V., Moore B., Bower R., 2000, Science, 288, 1617
- Read J. I., Wilkinson M. I., Evans N. W., Gilmore G., Kleyna J. T., 2006, MNRAS, 366, 429
- Roediger E., Brüggen M., 2006, MNRAS, 369, 567
- Roediger E., Hensler G., 2005, A&A, 433, 875
- Sánchez-Janssen R., Aguerri J. A. L., Muñoz-Tuñón C., 2008, ApJ, 679, L77
- Sawala T., Scannapieco C., White S., 2011, ArXiv e-prints
- Springel V., 2005, MNRAS, 364, 1105
- Tecce T. E., Cora S. A., Tissera P. B., 2011, MNRAS, 416, 3170
- van Dokkum P. G., Franx M., Kelson D. D., Illingworth G. D., Fisher D., Fabricant D., 1998, ApJ, 500, 714
- Villalobos Á., Helmi A., 2008, MNRAS, 391, 1806
- Wang L., Li C., Kauffmann G., De Lucia G., 2007, MNRAS, 377, 1419
- Weinmann S. M., Lisker T., Guo Q., Meyer H. T., Janz J., 2011a, MNRAS, 416, 1197
- Weinmann S. M., van den Bosch F. C., Pasquali A., 2011b, ArXiv e-prints
- Weinmann S. M., van den Bosch F. C., Yang X., Mo H. J., 2006, MNRAS, 366, 2
- Wetzel A. R., White M., 2010, MNRAS, 403, 1072
- White S. D. M., 1976, MNRAS, 177, 717
- Wilman D. J., Oemler Jr. A., Mulchaey J. S., McGee S. L., Balogh M. L., Bower R. G., 2009, ApJ, 692, 298
- Yang X., Mo H. J., van den Bosch F. C., 2009, ApJ, 695, 900
- Zabludoff A. I., Mulchaey J. S., 1998, ApJ, 496, 39
- Zhao D. H., Mo H. J., Jing Y. P., Börner G., 2003, MNRAS, 339, 12

APPENDIX A: FIGURES

The following Figures are included here for completeness and are the continuation of Figures 9, 10, 12, and 13. They illustrate the structural and kinematical evolution of disc galaxies for the remaining BUL, CIR, COL, MR1:5, MR1:20, MR1:10, and MR1:40 experiments, at the respective redshift epoch “ $z=0$ ” and “ $z=1$ ”.

This paper has been typeset from a $\text{\TeX}/\text{\LaTeX}$ file prepared by the author.

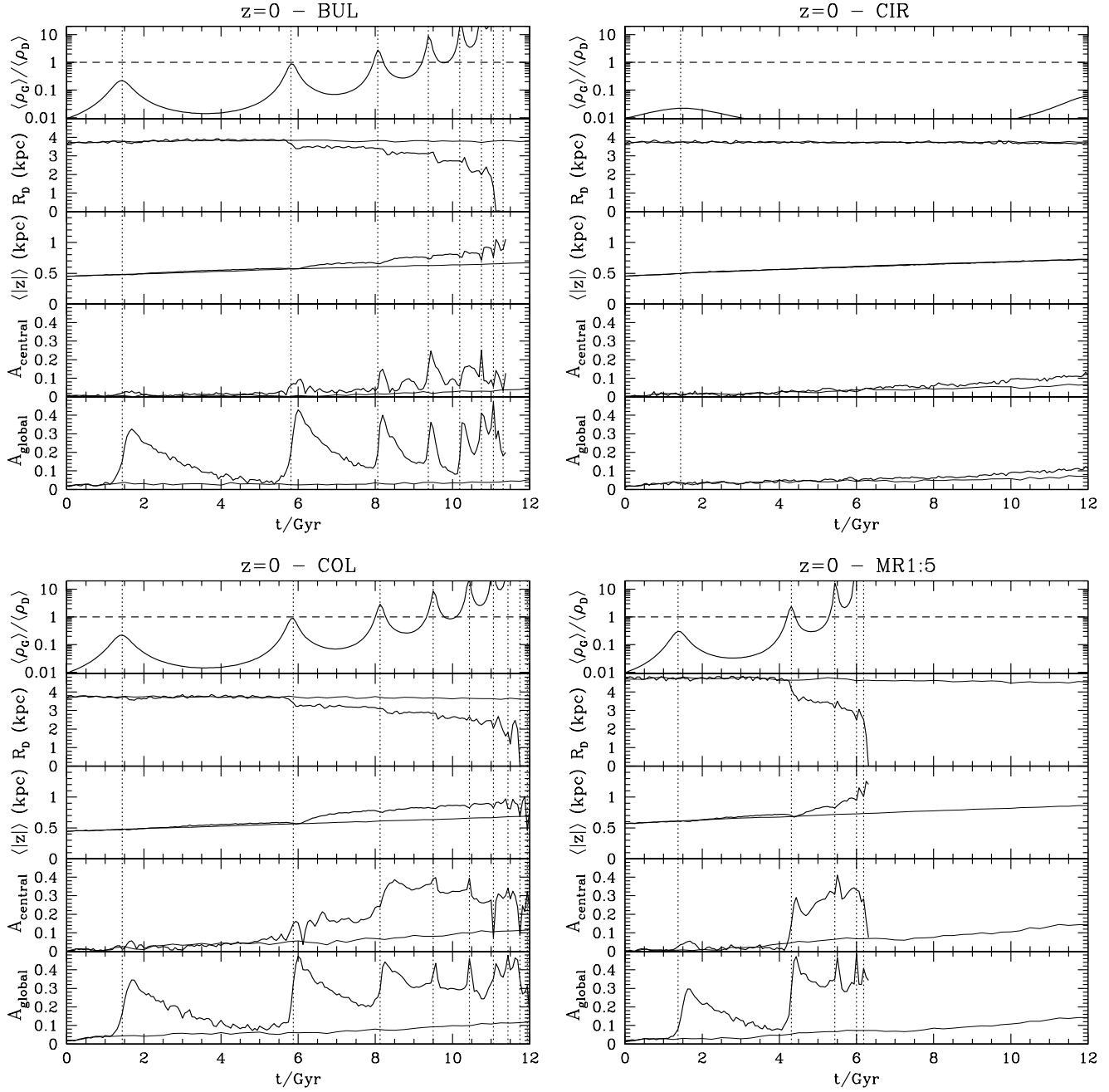


Figure A1. Continuation of Figure 9. Evolution of the structure of disc galaxies in terms of their scale-lengths, R_D , mean thickness, $\langle |z| \rangle$, and both central and global $m=2$ Fourier amplitudes, A_{central} and A_{global} . The evolution of discs is shown along with the strength of the global tidal force acting upon them along their orbits, estimated as the group-to-galaxy mean density ratio, $\langle \rho_{\text{group}} \rangle / \langle \rho_{\text{galaxy}} \rangle$ (see details in the text). For comparison, the evolution of the structure of isolated disc galaxies (thin lines), and the times of pericentric passages (vertical dotted lines), are also included.

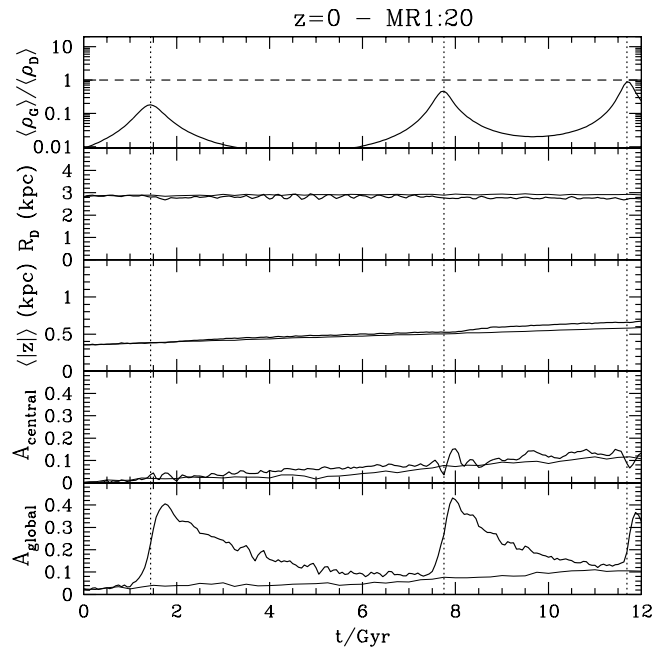


Figure A2. Same as Figure A1

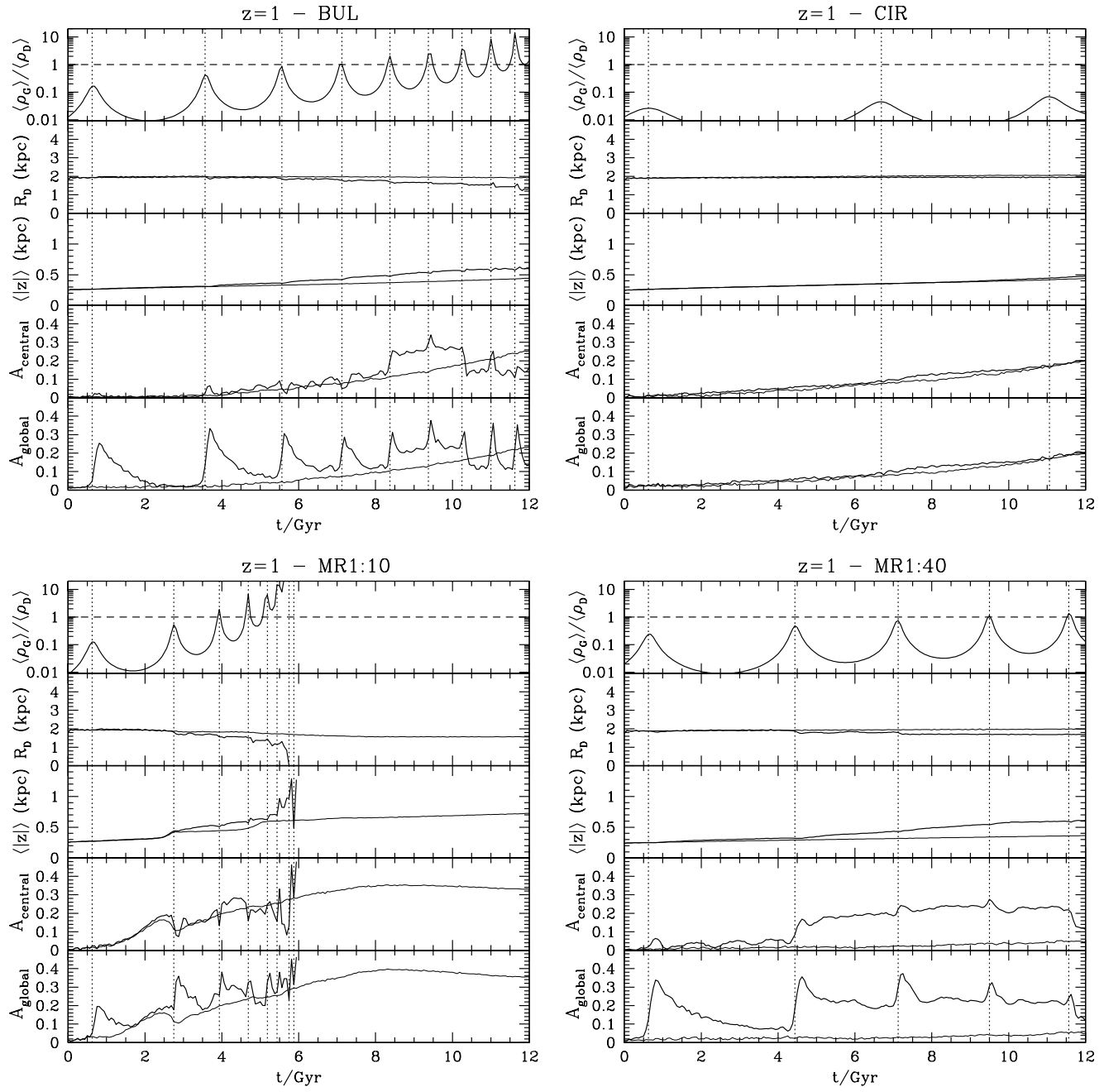


Figure A3. Continuation of Figure 10. Same description as Figure A1.

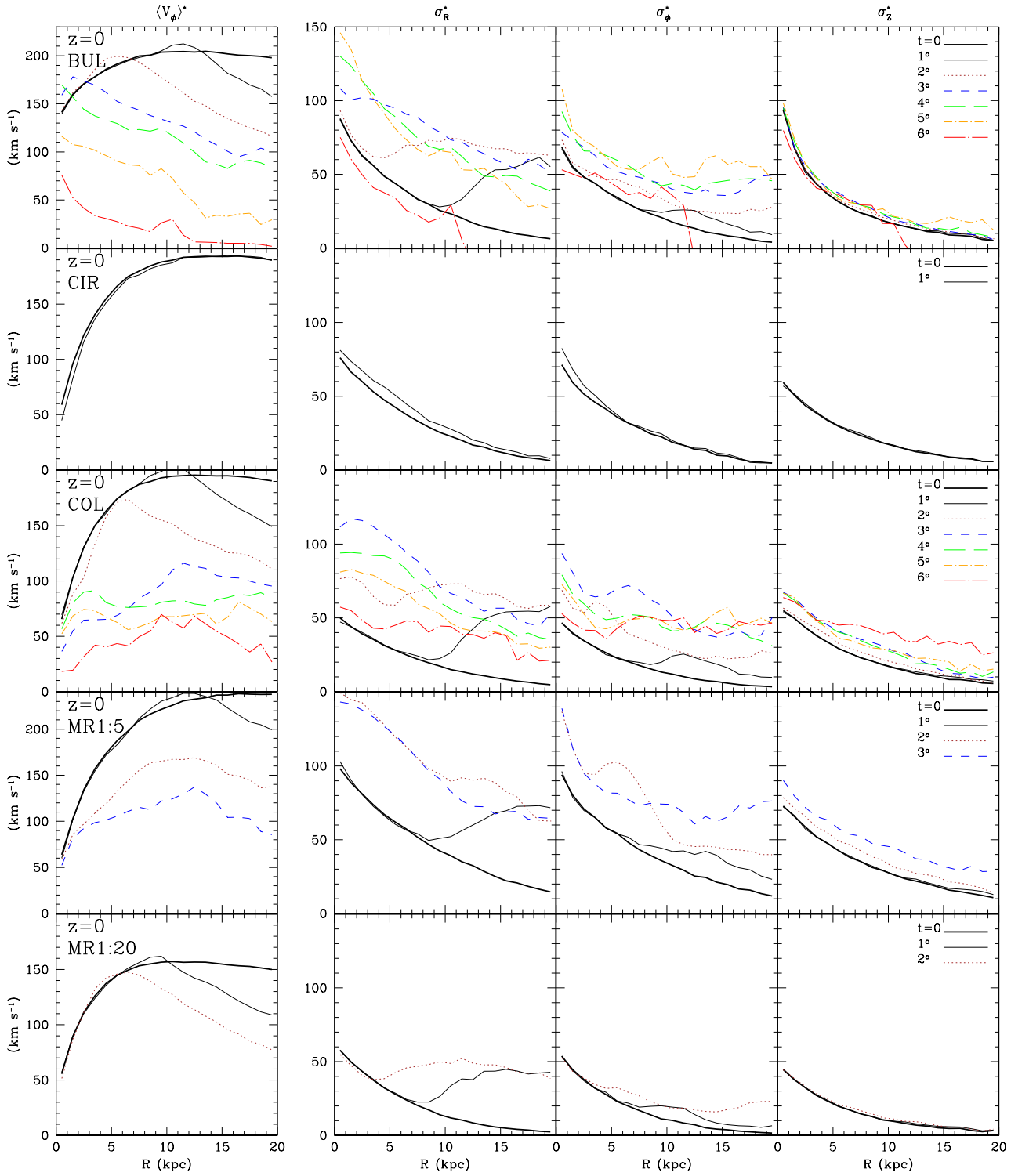


Figure A4. Continuation of Figure 12. Evolution of the kinematics of disc galaxies in terms of their mean rotation, $\langle V_\phi \rangle$, and the radial, azimuthal and vertical components of their velocity dispersions, σ_R , σ_ϕ , and σ_z respectively, after each of their first six pericentric passages. The kinematics of discs have been computed in concentric rings, 1 kpc wide, considering only stars that remain bound and are located within 3 kpc from the midplane, and have been corrected by the evolution of the respective disc in isolation.

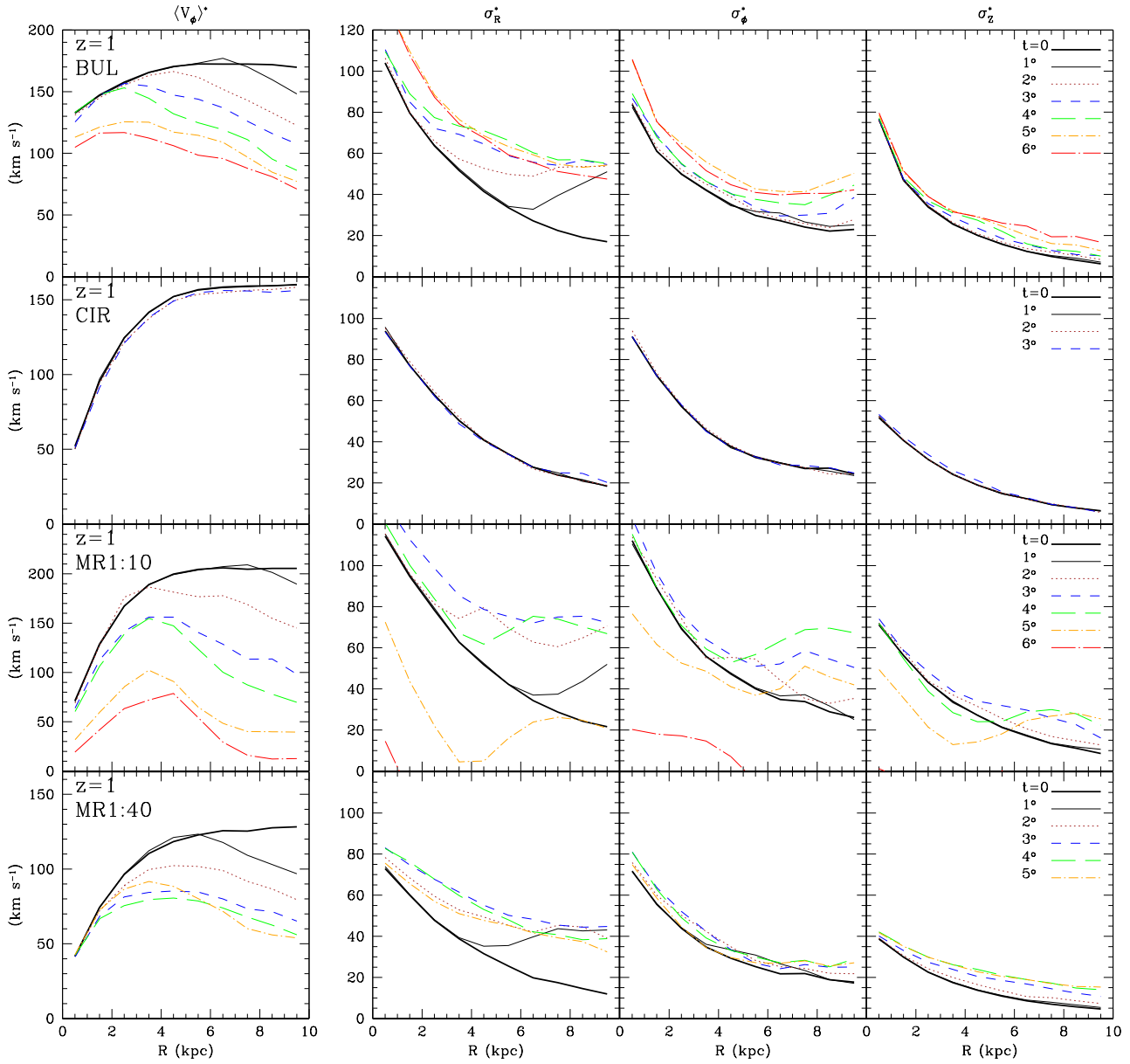


Figure A5. Continuation of Figure 13. Same description as Figure A4.

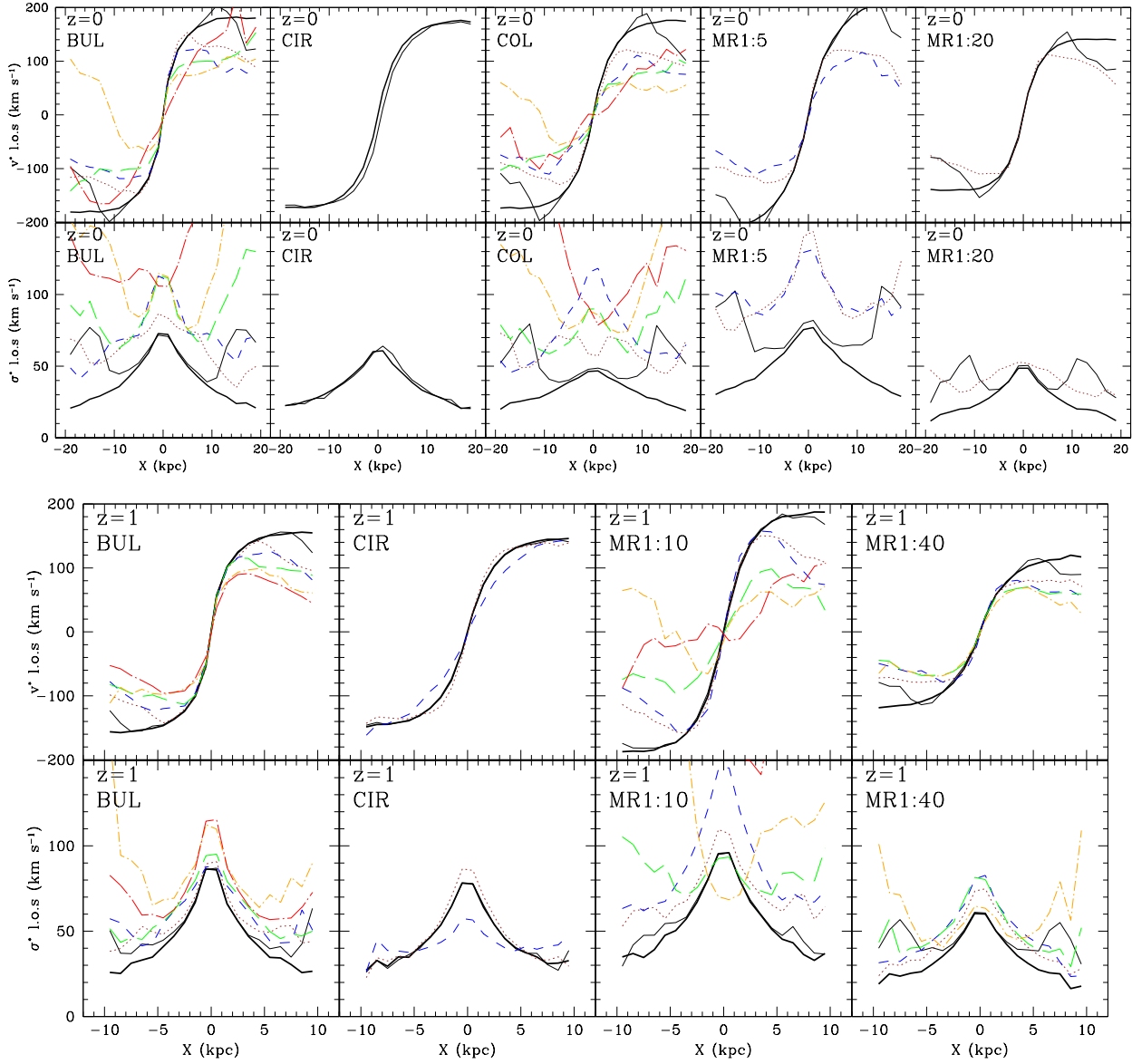


Figure A6. Continuation of Figure 14. Evolution of the kinematics of disc galaxies in terms of their line-of-sight velocities and velocity dispersions, after each of their first six pericentric passages. All discs are placed edge-on, with their midplanes along the X-axis. The kinematics have been computed in 1 kpc-wide bins along the X-axis, considering *all* disc stars (both bound and unbound) located within 3 kpc from the midplane, and have been corrected by the evolution of the respective disc in isolation. The line types and colour code are as in Figures A4 and A5.